SIAM J. FINANCIAL MATH.
Vol. 6, pp. 559–593

Consistent Pricing of Options on Leveraged ETFs*

Andrew Ahn†, Martin Haugh†, and Ashish Jain‡

Abstract. We consider the problem of pricing options on a leveraged ETF (LETF) and the underlying ETF in a model-consistent manner. We show that if the underlying ETF has Heston dynamics, then the LETF also has Heston dynamics so that options on both the ETF and the LETF can be priced analytically using standard transform methods. If the underlying ETF has tractable jump-diffusion dynamics, then the dynamics of the corresponding LETF are generally intractable in that we cannot compute a closed-form expression for the characteristic function of the log-LETF price. In that event we either (i) evaluate the appropriate transform numerically or (ii) propose tractable approximations based on either moment-matching techniques or saddlepoint approximations to the LETF price dynamics under which the transform can be found in closed form. In a series of numerical experiments including both low- and high-volatility regimes, we show that the resulting LETF option price approximations are very close to the true prices which we calculate via Monte Carlo. Because approximate LETF option prices can be computed very quickly, our methodology should be useful in practice for pricing and risk-managing portfolios that contain options on both ETFs and related LETFs. Our numerical results also demonstrate the model dependency of LETF option prices, and this is particularly noticeable in high-volatility environments.

Key words. options, transforms, leveraged ETF

AMS subject classifications. 91G20, 91G60

DOI. 10.1137/151003933

1. Introduction.

According to industry sources, as of April 2015 there were more than 5,500 registered ETFs globally with assets under management (AUM) of approximately $3 trillion. These ETFs are spread among many asset classes, including equity, fixed income, commodity, and foreign exchange. There were liquid options available on approximately 500 of these ETFs in 2013, and these ETFs accounted for approximately $1.9 trillion of the $3 trillion in AUM. Moreover the total ETF options volume is very large indeed: according to the Chicago Board Options Exchange [9], of the 4.1 billion exchange traded options contracts in 2013, 1.45 billion were ETF options, with equity options and cash index options accounting for 2.27 billion and 0.39 billion, respectively. In contrast, there were approximately 2 billion contracts traded in 2006, with a split of 1.5 billion equity options, 350 million ETF options, and 180 million cash index options. Between 2006 and 2010 the ETF options market therefore grew by a factor of four and is now a very large market indeed.

An even more recent development has been the introduction of *leveraged* ETFs (LETFs). An LETF is an exchange-traded derivative security based on a single underlying ETF or

*Received by the editors January 14, 2015; accepted for publication (in revised form) May 28, 2015; published electronically July 23, 2015.
http://www.siam.org/journals/sifin/6/100393.html

†Department of IE and OR, Columbia University, New York, NY 10027 (aja2133@columbia.edu, mh2078@columbia.edu).
‡New York, NY (ashish.jain8@gmail.com).

index. It is intended to achieve a *daily* return of ϕ times the daily return of the underlying ETF, and the LETF manager needs to rebalance his portfolio on a daily basis in order to achieve this. The constant ϕ is known as the *leverage ratio* of the LETF. As of 2010, there were approximately 150 LETFs with a total of \$30 billion in AUM, and approximately 100 of these LETFs have liquid options traded on them. Moreover, a given LETF typically has a very large and liquid ETF or index as its underlying security with options traded on both the LETF and the underlying ETF.

Upon their introduction, there was considerable confusion among investors over the performance of LETFs, particularly during the financial crisis when volatility levels spiked to unprecedented levels. In particular, many investors did not appreciate that LETFs had a negative exposure to the realized variance of the underlying ETF and therefore did not anticipate their potentially poor performance during this period. Cheng and Madhavan [7] and Avellaneda and Zhang [2] were the first to model and explain this LETF performance. In a continuous-time diffusion framework they obtained an expression (see (2.2) below) that highlighted this negative exposure to realized variance. Based on results by Haugh and Jain in [14], Haugh [13] also derived this expression as a simple case of a more general expression for the realized wealth that results from following a constant proportion trading strategy in a multisecurity diffusion setting.

While these papers helped to explain LETF performance, there has been little work on the pricing of LETF options and, in particular, on pricing them in a manner that is *consistent* with the pricing of options on the underlying ETF. One approach for pricing LETF options is based on using the Black–Scholes formula with the implied volatility taken from a related ETF option and then scaled by the leverage ratio. But this approach is ad hoc and has not been properly justified. Concurrent with our work is the recent paper of Leung and Sircar [16], who use asymptotic techniques in a multiscale stochastic volatility diffusion setting to understand the link between implied volatilities of the underlying ETF and related LETFs of a given leverage ratio. They then use the resulting insights to identify possible mispricings in the marketplace.

In this paper we price LETF options quickly and *consistently* with options on the underlying ETF under three different models: (i) Heston's [15] stochastic volatility model, (ii) the Bates [4] jump-diffusion model, and (iii) an affine jump-diffusion (AJD) model of Duffie, Pan, and Singleton [8], which includes jumps in both the volatility and price processes. In what follows, we will often refer to these models as the SV, SVJ, and SVCJ models, respectively. It should also be clear that the approximation techniques we develop in this paper can be applied more generally and that our treatments of the SV, SVJ, and SVCJ models may be viewed as applications of a more general approach. For example, other AJD models of Duffie et al. [8] should also be amenable to our approximation techniques. We do not propose a "one size fits all" approximation, however, so some additional work will generally be required to obtain a suitable approximation for a new set of underlying ETF price dynamics.

We show that if the underlying ETF has Heston dynamics, then the LETF also has Heston dynamics, so that options on both the ETF and the LETF can be priced analytically using standard transform methods. If the underlying ETF has tractable jump-diffusion dynamics (as in (ii) and (iii) above), then the dynamics of the corresponding LETF are generally intractable in that we cannot compute a closed-form expression for the characteristic function of the log-

LETF price. Instead we can either compute this characteristic function numerically (as in (ii) above), or else (as in (iii) above) we construct tractable approximations to the LETF dynamics where the characteristic function of the log-LETF price can be found in closed form. Such approximations enables us to calculate approximate option prices very quickly. The key to this latter approach is that under our jump-diffusion models for the underlying ETF, the diffusion component of the LETF dynamics remains "tractable." We therefore only need to focus on approximating the jump component of the LETF dynamics.

The approximations that we propose include[1] classic moment-matching techniques and the saddlepoint approximation approach of Glasserman and Kim [10] for handling less tractable AJD processes. In a series of numerical experiments including both low- and high-volatility regimes, we show that the resulting LETF option price approximations are very close to the true prices which we calculate via Monte Carlo. Our approximate LETF option prices can be computed quickly and therefore should be useful in practice for pricing and risk-managing portfolios that contain options on both ETFs and related LETFs.

Our numerical experiments also show that the ratio of an LETF option implied volatility to the corresponding ETF option implied volatility can be far from the LETF leverage ratio. The difference between the two depends on whether or not the LETF is long or short and is model dependent, thereby emphasizing the path dependence of the LETF price at any given time. In order to illustrate just how model dependent the prices of LETF options can be, we also price these options under the Barndorff-Nielsen and Shephard [3] model in addition to the three models listed above. This model dependency calls into question the market practice of pricing an LETF option using the Black–Scholes formula with the strike and implied volatility scaled by the leverage ratio.

Finally, it is worth emphasizing that our use of the word "consistent" in the title of this paper refers to *model* or *internal* consistency. In particular, rather than using separate models for pricing ETF options and LETF options, our goal is to show how to consistently price these options at the model level only. We therefore do not claim that any one model can always price these options consistently with market prices. Indeed given the behavior of financial markets, we expect that the only models capable of always fitting to market prices are those models which have too many parameters and therefore tend to overfit. Moreover, given the need to frequently recalibrate even parsimonious models throughout the derivatives markets, we suspect that such models may never be found. Regardless, model-consistent pricing is a necessary step before one can tackle the problem of market-consistent pricing. Moreover, if the goal is to identify mispriced LETF options in the market, then model consistency rather than market consistency is clearly the appropriate approach.

The remainder of this paper is organized as follows. Section 2 describes our modeling assumptions for LETF price dynamics. In sections 3, 4, and 5 we consider the SV, SVJ, and SVCJ models, respectively, for the underlying ETF and describe how LETF options can

[1]Earlier versions of this paper proposed an approach where the entire distribution of the jump component of the LETF price dynamics was approximated by a more tractable distribution. While the resulting approximations were very accurate, the approach was very ad hoc and somewhat awkward to describe. We have therefore replaced it with approaches based on moment-matching and saddlepoint approximations. While both of these new approaches also require some work to implement, they are less ad hoc, easier to describe, and, as standard approximation techniques, easy to justify.

be calculated for each of these models. Section 6 describes how we calibrated these models, and section 7 provides numerical results confirming the quality of our moment-matching approximation for the SVCJ model. We describe the saddlepoint approximation approach in section 8, and we conclude in section 9. The appendices contain further details on our approximation methods as well as some additional numerical results.

2. Modeling leveraged ETF dynamics. We let S_t and L_t denote the time t prices of the underlying ETF and LETF, respectively. Rather than working in discrete time we will work instead in continuous time and assume that the LETF is rebalanced continuously.

Modeling leveraged ETF dynamics when the underlying has diffusion dynamics. If S_t follows a diffusion, then the mechanics of the LETF implies that L_t has dynamics

$$\frac{dL_t}{L_t} = \phi \cdot \frac{dS_t}{S_t} + (1-\phi)r\,dt - f\,dt, \tag{2.1}$$

where r is the continuously compounded risk-free interest rate and f is the constant expense ratio of the LETF. There is no difficulty incorporating dividends as long as we interpret the dS_t term in (2.1) to include any dividend payments. The $(1-\phi)r\,dt$ term in (2.1) reflects the cost of funding the leveraged position when $\phi > 1$, or the risk-free income from an inverse ETF when $\phi < 0$.

Assuming general diffusion dynamics of the form $dS_t = \mu_t S_t\,dt + \sigma_t S_t\,dW_t$, Avellaneda and Zhang [2] solved[2] (2.1) to obtain

$$\frac{L_T}{L_0} = \left(\frac{S_T}{S_0}\right)^{\phi} \exp\left((1-\phi)rT - fT + \frac{1}{2}\phi(1-\phi)\int_0^T \sigma_t^2 dt\right). \tag{2.2}$$

They used this expression to explain the empirical performance of LETFs during the financial crisis. Note that for leverage ratios satisfying $|\phi| > 1$ it is clear from (2.2) that a long LETF position is short realized variance for a given value of S_T. Haugh and Jain [14] also derived a more general form of (2.2) in a dynamic portfolio optimization context. It is also easy to show that this negative exposure to variance could be interpreted as a (multiplicative) premium that must be paid for obtaining a payoff of $(S_T/S_0)^{\phi}$ rather than the payoff you would obtain from a buy-and-hold portfolio with initial leverage of ϕ.

Modeling leveraged ETF dynamics when the underlying can jump. Note also that if S_t can jump, then (2.1) will still be valid as long as we truncate the jumps appropriately to reflect the limited liability of the LETF. But of course the LETF manager must implicitly pay for the truncation of these jumps, since otherwise an arbitrage opportunity would exist. When the underlying price process can jump, we therefore assume dynamics for L_t of the form

$$\frac{dL_t}{L_{t-}} = \phi \cdot \frac{dS_t^*}{S_{t-}} + (1-\phi)r\,dt - f\,dt - c_t\,dt, \tag{2.3}$$

where dS_t^* denotes the possibly truncated increment in the underlying price at time t, and $c_t\,dt$ is the "insurance premium" paid at time t to insure against L_t violating limited liability

[2] Cheng and Madhavan [7] obtained (2.2) under geometric Brownian motion dynamics.

in the next dt units of time. Note that we can also write (2.3) more explicitly as

$$\frac{dL_t}{L_{t-}} = \phi \cdot \frac{dS_t}{S_{t-}} + (1-\phi)r dt - f dt - c_t dt \quad \text{for } 0 \le t < \tau, \tag{2.4}$$

where τ is the first-passage time of the event $\phi\, dS_t/S_{t-} \le -1$. Moreover we assume $L_t \equiv 0$ for all $t \ge \tau$.

2.1. Risk-neutral dynamics for the leveraged ETF. While not stated explicitly, the dynamics in (2.1) to (2.4) are assumed to hold under P, the objective or true data-generating probability measure. Because these are pathwise dynamics they must therefore hold under any equivalent martingale measure, Q. In this paper we will take Q to be the martingale measure associated with taking the cash account as numeraire. We will also assume that the risk-free rate, r, is a constant[3] but note that it would be straightforward to relax this assumption if necessary. Note that once we specify Q-dynamics for S_t we are also implicitly specifying Q-dynamics for L_t via (2.3) and (2.4).

All of our examples in this paper will assume that the underlying security price has risk-neutral dynamics of the form

$$\frac{dS_t}{S_{t-}} = (r - q - \lambda m)dt + \sqrt{V_t} dW_t^S + dJ_t, \tag{2.5}$$

where q is the dividend yield, λ is the intensity of the jump process, J_t, and V_t is some stochastic volatility process. We will write $J_t := \sum_{i=1}^{N_t}(Y_i - 1)$ so that $Y_i - 1$ represents the relative jump size in the security price at the time of the ith jump. In particular, if the ith jump occurs at time τ_i, then $S_{\tau_i} = S_{\tau_i -} Y_i$. We set $m = \mathbb{E}^Q(Y_i - 1)$, which guarantees that the discounted gains process associated with holding the underlying security is a Q-martingale.

Some simple algebra confirms that jumps, Y_i, in the underlying security that satisfy $\phi(Y_i - 1) < -1$ would cause L_t to go negative in the absence of limited liability. In the presence of limited liability we must therefore use a jump process for L_t of the form $J_t^L := \sum_{i=1}^{N_t}(Y_i^L - 1)$, where

$$Y_i^L := \max\left(\phi(Y_i - 1),\ -1\right) + 1.$$

Continuing our insurance analogy, we could imagine the leveraged ETF manager being exposed to all jumps, $\phi(Y_i - 1)$, but in such a way that he is insured against any jumps that would cause L_t to go negative. We can calculate the premium per unit time, c_t, as the (risk-neutral) expected loss per unit time that the insurer would incur due to a possible jump in L_t to a negative value. The risk-neutral value of this insurance[4] is then given by

$$\begin{aligned} c_t &:= \lambda p^* \left(\mathbb{E}^Q[-1 - \phi(Y_i - 1) \,|\, \phi(Y_i - 1) < -1]\right) \\ &= -\lambda p^* \left(\mathbb{E}^Q[\phi(Y_i - 1) \,|\, \phi(Y_i - 1) < -1] + 1\right), \end{aligned} \tag{2.6}$$

where $p^* := Q(\phi(Y_i - 1) < -1)$, so that λp^* is the arrival rate for jumps that will drive L_t to zero. The "+1" term on the right-hand side of (2.6) is required because the insurance only

[3] Given the short expirations that are typical for LETF options, the assumption of constant interest rates is easy to justify.

[4] Because λ is a constant in our examples, c_t is in fact a constant. We could, however, also use our approach for more general point processes such as affine processes, which are also tractable.

covers that part of the jump *beyond* -1, and indeed the jump event itself will drive the LETF price, L_t, to 0. Substituting (2.6) and (2.5) into (2.4) and also taking the insurance payoff, dJ_t^{ins} say, into account, we obtain the following risk-neutral dynamics for L_t:

$$\frac{dL_t}{L_{t-}} = \phi\left((r-q-\lambda m)dt + \sqrt{V_t}dW_t^S + dJ_t\right) + (1-\phi)rdt - fdt - c_t dt + dJ_t^{ins} \tag{2.7}$$

$$= (r - \phi q - f - \lambda\phi m)dt + \phi\sqrt{V_t}dW_t^S + dJ_t^L - c_t dt$$

$$= (r - \phi q - f - \lambda m_L)dt + \phi\sqrt{V_t}dW_t^S + dJ_t^L, \tag{2.8}$$

where we have used the fact that $\phi dJ_t + dJ_t^{ins} = dJ_t^L$ and used (2.6) and $m = \mathbb{E}^Q(Y_i - 1)$ to obtain

$$\begin{aligned} m_L &:= \phi m + c_t/\lambda \\ &= (1-p^*)\cdot\mathbb{E}^Q[\phi(Y_i-1)|\phi(Y_i-1) > -1] - p^*. \end{aligned} \tag{2.9}$$

Note that these dynamics are only valid for $0 \le t \le \tau$ and that (2.7) does not contradict (2.4) since the dJ_t^{ins} term (which is absent in (2.4)) is only nonzero at time τ.

In the foregoing analysis we have implicitly assumed that dividends from the underlying ETF (or index) will be multiplied by ϕ and then paid out, in the case where ϕ is positive, to investors in the corresponding LETF. If ϕ is negative, then the LETF investor will have to pay out these dividends. We make this assumption in order to simplify the exposition but note that in practice the treatment of dividends can vary with each LETF. For example, inverse LETFs with $\phi < 0$ typically have a dividend yield of zero and do not require their investors to make dividend payments, while positively leveraged ETFs typically pay a smaller dividend than ϕq. Moreover, because leveraged ETFs often have other sources of income, e.g., interest income from the proceeds of short sales, understanding dividend dynamics needs to be done on a case-by-case basis. We do note that it is also possible to infer an implied LETF dividend yield in the usual manner using put-call parity. For the purpose of this paper, however, we will assume a dividend yield of $\phi q + f$ as implied by (2.8) and simply note that it would be straightforward to handle other dividend assumptions.

The path dependence of leveraged ETF prices. While clear from (2.2) in the case of a diffusion, it is worth emphasizing that the risk-neutral dynamics of (2.8) yield a terminal value of L_T that is path dependent. In particular L_T cannot be expressed as a function of S_T alone, and so pricing an option on L_T does not amount to simply pricing some derivative of S_T. (Pricing a derivative of S_T can be done in a model-independent fashion by using the implied volatility surface of S_T to compute the risk-neutral marginal distribution of S_T.)

3. Heston's stochastic volatility model.

The first model that we consider is Heston's [15] stochastic volatility (SV) model, and we will see that it is particularly easy to price LETF options under this model. We assume the underlying ETF price, S_t, has risk-neutral dynamics given by

$$\frac{dS_t}{S_t} = (r-q)dt + \sqrt{V_t}dW_t^S, \tag{3.1}$$

$$dV_t = \kappa(\theta - V_t)dt + \gamma\sqrt{V_t}dW_t^V, \tag{3.2}$$

where q is the dividend yield, and W_t^S and W_t^V are standard Brownian motions with constant correlation parameter, ρ. Our first result is particularly straightforward and states that if S_t has Heston dynamics, then so too does L_t.

Proposition 1. *Suppose the underlying ETF price, S_t, has Heston dynamics given by (3.1) and (3.2). Then assuming a leverage ratio of ϕ, the LETF price, L_t, has dynamics given by*

$$\frac{dL_t}{L_t} = (r - q_L)dt + sign(\phi) \cdot \sqrt{V_t^L} dW_t^S, \tag{3.3}$$

$$dV_t^L = \kappa_L(\theta_L - V_t^L)dt + \gamma_L \sqrt{V_t^L} dW_t^V, \tag{3.4}$$

where $V_t^L := \phi^2 V_t$, $q_L := \phi q + f$, $\kappa_L := \kappa$, $\gamma_L := |\phi|\gamma$, and $\theta_L := \phi^2\theta$. In particular the LETF also has Heston dynamics.

Proof. Since S_t follows a diffusion, we note that (2.1) and (2.3) are identical. If we therefore substitute (3.1) into (2.3), we obtain $dL_t/L_t = (r - \phi q)dt + \phi\sqrt{V_t}dW_t^S$, which immediately yields (3.3). Similarly, using (3.2) we obtain $dV_t^L = \phi^2\kappa(\theta - V_t)dt + \phi^2\gamma\sqrt{V_t}dW_t^V$, which yields (3.4). ∎

Proposition 1 shows that if S_t has Heston dynamics with parameter set $(q, \kappa, \gamma, \theta, V_0, \rho)$, then L_t has Heston dynamics with parameter set

$$(q_L, \kappa_L, \gamma_L, \theta_L, V_0^L, \rho_L) := (\phi q + f, \kappa, |\phi|\gamma, \phi^2\theta, \phi^2 V_0, \text{sign}(\phi) \cdot \rho). \tag{3.5}$$

Since it is easy to price options using transform methods under the Heston model, Proposition 1 implies that we can price options on ETFs and LETFs consistently with each other when the ETF has Heston dynamics. While this result was very easy to derive, we have not seen it elsewhere in the literature. In his Ph.D. thesis, for example, Zhang [18] considers the pricing of LETF options when the underlying has Heston dynamics. He does not observe that L_t also has Heston dynamics, however, probably because he worked with (2.2) rather than (2.1). Indeed Zhang proposed a change of measure motivated by (2.2) and observed that L_t had Heston dynamics with time-dependent parameters under this new measure. The time dependency of the parameters under the new measure does not allow options on the LETF to be calculated via transform methods, however.

One further remark is in order at this point. It should be clear that the tractability that the LETF dynamics inherits from the underlying price dynamics will hold for diffusions in general and not just the Heston model. This should be clear from (2.1).

4. The SVJ model.

The Bates [4] stochastic volatility (SVJ) model is an extension of the SV model that allows for the possibility of jumps in the security price process. The risk-neutral dynamics for the SVJ model are

$$\frac{dS_t}{S_{t-}} = (r - q - \lambda m)dt + \sqrt{V_t}dW_t^S + dJ_t, \tag{4.1}$$

$$dV_t = \kappa(\theta - V_t)dt + \gamma\sqrt{V_t}dW_t^V, \tag{4.2}$$

where W_t^S and W_t^V are standard Brownian motions with correlation coefficient ρ, N_t is a Poisson process with intensity λ, and $J_t := \sum_{i=1}^{N_t}(Y_i - 1)$ so that $Y_i - 1$ represents the relative

jump size in the security price at the time of the ith jump. In particular, if the ith jump occurs at time τ_i, then $S_{\tau_i} = S_{\tau_i -} Y_i$. The Y_i's are assumed to be independent and identically log-normally distributed with $\log Y_i \sim \mathrm{N}(a, b^2)$ with $m := \mathbb{E}(Y_i - 1) = \exp\left(a + \frac{b^2}{2}\right) - 1$.

Proposition 2. *If S_t has risk-neutral dynamics given by (4.1) and (4.2), then the risk-neutral dynamics of L_t satisfy*

$$\frac{dL_t}{L_{t-}} = (r - q_L - \lambda m_L)dt + sign(\phi)\sqrt{V_t^L}\, dW_t^S + dJ_t^L, \tag{4.3}$$

$$dV_t^L = \kappa_L(\theta_L - V_t^L)dt + \gamma_L\sqrt{V_t^L}\, dW_t^V, \tag{4.4}$$

where $V_t^L := \phi^2 V_t$, $q_L := \phi q + f$, $\kappa_L := \kappa$, $\gamma_L := |\phi|\gamma$, $\theta_L := \phi^2\theta$, and $J_t^L := \sum_{i=1}^{N_t}(Y_i^L - 1)$, where

$$\begin{aligned} Y_i^L &:= \max\left(\phi(Y_i - 1),\ -1\right) + 1, \\ m_L &:= (1 - p^*) \cdot \mathbb{E}^Q[\phi(Y_i - 1) | \phi(Y_i - 1) > -1] - p^*, \\ \text{and} \quad p^* &:= Q(\phi(Y_i - 1) < -1) = \begin{cases} F\left(\log\left(\frac{\phi-1}{\phi}\right); a, b\right) & \text{if } \phi > 0, \\ 1 - F\left(\log\left(\frac{\phi-1}{\phi}\right); a, b\right) & \text{if } \phi < 0, \end{cases} \end{aligned} \tag{4.5}$$

where $F(\,\cdot\,; a, b)$ is the cumulative distribution function of the $N(a, b)$ distribution.

Proof. Equation (4.3) follows from (2.8). Since $V_t^L := \phi^2 V_t$ it is also clear that (4.4) follows directly from (4.2). ∎

We would like to price options on the LETF using standard transform methods based on calculating the characteristic function of the log-LETF price. But first we will distinguish between two types of jumps. We say that a jump, Y, is of type I if it satisfies $\max(\phi(Y-1)+1, 0) = 0$. Such a jump would drive L_t to zero. Otherwise, it is of type II. A jump is type I with probability p^* and type II with probability $1 - p^*$, where p^* is defined in (4.5). Let $N_1(t)$ and $N_2(t)$ denote, respectively, the number of type I and type II jumps occurring in $[0, t]$. By the thinning property of Poisson processes, $N(t) = N_1(t) + N_2(t)$, where $N_1(t)$ and $N_2(t)$ are independent Poisson processes with rates λp^* and $\lambda(1 - p^*)$, respectively. We then have the following proposition.

Proposition 3. *Let $C(L_0, K, T)$ be the time $t = 0$ price of a call option on the LETF with strike K, maturity T, and initial LETF price L_0. Then $C(L_0, K, T) = \exp(-\lambda p^* T)\, \hat{C}(L_0, K, T)$, where*

$$\hat{C}(L_0, K, T) \ := \ \mathbb{E}_0^Q[e^{-rT}(L_T - K)^+ | N_1(T) = 0] \tag{4.6}$$

is the value of the option given that there are no type I jumps in $[0, T]$.

Proof. The proof is immediate once we note that a type I jump will cause the LETF price to immediately fall to zero so that the call option will expire worthless in that event. ∎

We will compute LETF call option prices[5] in the SVJ model by computing $\hat{C}(L_0, K, T)$ and then using Proposition 3. We would like to compute $\hat{C}(L_0, K, T)$ using numerical transform

[5]Put prices can then be obtained from put-call parity.

inversion methods[6] applied to the characteristic function of the log-LETF price, L_t, conditional on $N_1(T) = 0$. Since the diffusion component of the LETF dynamics is Heston (and therefore easy to handle), the only difficulty is in computing the characteristic function of the jump component of the log-LETF price conditional on $N_1(T) = 0$.

Toward this end, let $\Phi_{J_2^L(T)}$ denote the characteristic function of the jump component of the log-LETF price conditional on $N_1(T) = 0$. Then a standard expression for the characteristic function of a compound Poisson process yields

$$\begin{aligned}\Phi_{J_2^L(T)}(u) &= \mathbb{E}_0^Q\left[\exp\left(iu\cdot\sum_{j=1}^{N(T)}\log(Y_j^L)\right)\,\middle|\,N_1(T)=0\right]\\ &= \mathbb{E}_0^Q\left[\exp\left(iu\cdot\sum_{j=1}^{N_2(T)}\log(Y_j^L)\right)\right]\\ &= \exp\left[\lambda(1-p^*)T\left(\Phi_X(u)-1\right)\right],\end{aligned}\tag{4.7}$$

where $\Phi_X(\cdot)$ is the characteristic function of X with

$$X := \left(\log(\phi(Y-1)+1)\mid \phi(Y-1)+1>0\right).\tag{4.8}$$

If we can calculate $\Phi_X(\cdot)$, then it is easy to see that the characteristic function of the log-LETF price conditional on $N_1(T) = 0$ is given by

$$\Phi_L^{N_1\equiv 0}(u) := \exp(-\lambda m_L iuT)\,\Phi_T^{SV}(u\,;r,q_L,\kappa_L,\gamma_L,\theta_L,V_0^L,\rho_L,L_0)\times\exp\left[\lambda(1-p^*)T(\Phi_X(u)-1)\right].\tag{4.9}$$

We could then use (4.9) together with the Carr–Madan [6] approach to compute $\hat{C}(L_0,K,T)$ in (4.6) and therefore obtain our LETF call option prices. We cannot compute $\Phi_X(\cdot)$ analytically, however, and so we must compute it numerically. Since the density function of X is known,[7] we can compute $\Phi_X(u)$ for a given u via numerical integration. Our approach then is to precalculate $\Phi_X(u)$ on a fine grid $u = u_1,\ldots,u_N$, and then for an arbitrary u we will approximate $\Phi_X(u)$ with $\Phi_X(u_j)$, where u_j is the closest grid-point to u. Using a suitably fine grid, we can obtain a very good approximation to $\Phi_X(\cdot)$ which in turn yields a very accurate approximation, $\hat{\Phi}_L^{N_1\equiv 0}(\cdot)$, that we can use in place of (4.9).

5. The SVCJ model.

The stochastic volatility model (SVCJ) with contemporaneous jumps in price and variance was introduced by Duffie, Pan, and Singleton [8]. The risk-neutral dynamics for this model are

$$\frac{dS_t}{S_{t-}} = (r-q-\lambda m)dt + \sqrt{V_t}dW_t^S + dJ_t^S,\tag{5.1}$$

[6] We use the Carr–Madan [6] Fourier inversion approach throughout the paper.

[7] We can define X as $X := [g(\log(Y_i)) \mid \phi(Y_i-1)+1>0]$, where $g(x) := \log(\phi(e^x-1)+1))$. Letting $f(\cdot;a,b)$ denote the density of $\log(Y)\sim \mathrm{N}(a,b)$, we obtain

$$q(x) = \frac{f(g^{-1}(x);a,b)}{\mathbb{P}(\phi(Y_i-1)+1>0)}\cdot\left|\frac{d}{dx}(g^{-1}(x))\right| = \frac{\mathrm{sign}(\phi)}{1-p^*}\cdot f\left(\log\left(\frac{e^x+\phi-1}{\phi}\right);a,b\right)\cdot\frac{e^x}{e^x+\phi-1}$$

as the density of X.

$$dV_t = \kappa(\theta - V_t)dt + \gamma\sqrt{V_t}dW_t^V + dJ_t^V, \tag{5.2}$$

where $J_t^S := \sum_{i=1}^{N_t}(Y_i - 1)$, $J_t^V := \sum_{i=1}^{N_t} Z_i$, and N_t is a Poisson process with intensity λ. As before, $Y_i - 1$ represents the percentage change in the security price due to the ith jump size and Z_i is the corresponding change in variance. In particular if the ith jumps occur at time τ_i, then $S_{\tau_i} = S_{\tau_i -} Y_i$ and $V_{\tau_i} = V_{\tau_i -} + Z_i$. We also assume the jumps in security price and variance are correlated. More precisely, we assume the Z_i's are exponentially distributed with mean μ_v and that, conditional on Z_i, $\log(Y_i)$ is normally distributed with mean $a + \rho_J Z_i$ and variance b^2. In other words,

$$Z_i \sim \text{Exp}(\mu_v^{-1}) \tag{5.3}$$

and

$$\log(Y_i) \;\sim\; \text{N}(a, b^2) + \rho_J Z_i \;\sim\; \text{N}(a, b^2) + \text{sign}(\rho_J) \cdot \text{Exp}(c), \tag{5.4}$$

where $c := |\rho_J \mu_v|^{-1}$ and the normal and exponential components in (5.4) are independent. We also have $\text{Corr}(Z_i, \log(Y_i)) = \text{sign}(\rho_J) \cdot ((bc)^2 + 1)^{-1/2}$, which approaches ± 1 as b goes to 0, and we see that $m = \mathbb{E}(Y_i - 1) = \exp\left(a + b^2/2\right) c/(c - \text{sign}(\rho_J)) - 1$. Finally note that W_t^S and W_t^V are standard Brownian motions with constant correlation coefficient ρ. We have the following proposition describing the risk-neutral dynamics of L_t in the SVCJ model.

Proposition 4. *If S_t has risk-neutral dynamics given by (5.1) and (5.2), then the LETF with leverage ratio ϕ has risk-neutral dynamics*

$$\frac{dL_t}{L_{t-}} = (r - q_L - \lambda m_L)dt + sign(\phi)\sqrt{V_t^L}dW_t^S + dJ_t^L, \tag{5.5}$$

$$dV_t^L = \kappa_L(\theta_L - V_t^L)dt + \gamma_L\sqrt{V_t^L}dW_t^V + d(\phi^2 J_t^V), \tag{5.6}$$

where $V_t^L := \phi^2 V_t$, $q_L := \phi q + f$, $\kappa_L := \kappa$, $\gamma_L := |\phi|\gamma$, $\theta_L := \phi^2\theta$, $J_t^L := \sum_{i=1}^{N_t}(Y_i^L - 1)$, and

$$Y_i^L := \max\left(\phi(Y_i - 1),\; -1\right) + 1,$$

$$p^* := Q(\phi(Y_i - 1) < -1) = \begin{cases} P\left(\log(Y_i) < \log\left(\frac{\phi-1}{\phi}\right)\right) & \text{if } \phi > 0, \\ P\left(\log(Y_i) > \log\left(\frac{\phi-1}{\phi}\right)\right) & \text{if } \phi < 0, \end{cases}$$

$$\text{and} \quad m_L := (1 - p^*) \cdot \mathbb{E}^Q[\phi(Y - 1)|\phi(Y - 1) > -1] - p^*. \tag{5.7}$$

Proof. Equation (5.5) follows directly from (2.8), and since $V_t^L := \phi^2 V_t$, (5.6) follows immediately from (5.2). ∎

The question that now arises is whether or not we can price options on the LETF with dynamics given by (5.5) and (5.6). We could try to use the approach we adopted for the SVJ model where we precomputed $\Phi_X(\cdot)$ on a fine grid of points, but this does not seem like a very promising approach for two reasons. First, X will be a bivariate random variable under the SVCJ model (see (5.8) below), and so we would need to precompute $\Phi_X(\cdot)$ on a two-dimensional grid. Second, and more importantly, under the SVCJ model the characteristic function of the log-LETF price must be computed as the solution of a series of ODEs (see

Appendix B.3) which depend in part on $\Phi_X(\cdot)$. Because this characteristic function is then used as an input to price LETF options via numerical transform inversion, it is desirable to have an analytic expression for it. Unfortunately we do not have an analytic expression for $\Phi_X(\cdot)$ under the SVCJ model.

We will therefore proceed by approximating the dynamics of the LETF with more tractable dynamics. But first note that if we define type I and type II jumps as before, then Proposition 3 remains valid under the SVCJ model so that (4.6) still holds, i.e., $C(L_0, K, T) = \exp(-\lambda p^* T)\ \hat{C}(L_0, K, T)$, where $\hat{C}(L_0, K, T) := \mathbb{E}_0^Q[e^{-rT}(L_T - K)^+ | N_1(T) = 0]$ is the value of the option given that there are no type I jumps in $[0, T]$. Our goal will be to approximate the option price by approximating $\hat{C}(L_0, K, T)$. To do this we let

$$\begin{aligned} X &:= (X_1, X_2) \\ &:= \left(\left(\log(\phi(Y_i - 1) + 1),\ \phi^2 Z_i\right)\ |\ \phi(Y_i - 1) + 1 > 0\right) \\ &= \left(\left(\log(Y_i^L),\ \phi^2 Z_i\right)\ |\ \phi(Y_i - 1) + 1 > 0\right) \end{aligned} \tag{5.8}$$

be the bivariate random vector representing jumps in the log-LETF price and its variance process, respectively. As stated above, we would like to have a closed-form expression for the characteristic function $\Phi_X(\cdot)$ of X so that we could then apply the methodology of Duffie, Pan, and Singleton [8] to compute the characteristic function of the log-LETF price.

We don't have such a closed-form expression, however, so we will instead approximate X with another bivariate distribution whose characteristic function is available in closed form. In particular, we will approximate X with a combination of univariate normal and bivariate exponential (BVE) distributions where the parameters of the approximating distribution will be chosen via a simple moment-matching procedure. Moment matching is a standard approximation approach and has been employed successfully in many domains, including (see, for example, Glasserman and Merener [12]) the pricing of financial derivatives. The specific details of the moment-matching algorithm are provided in Appendix B.2. As with many approximation approaches, it is necessary to tailor the approach to the problem at hand. In this case we have chosen the normal-BVE distribution to approximate X as defined for the SVCJ model, as we have found[8] it to be capable of providing a very good fit in this case. For other AJD models the normal-BVE distribution may not be suitable, and so it would be necessary[9] to use some other suitably tractable distribution.

6. Model calibration using synthetic data. We considered three different parameter sets for our numerical experiments. The first set was obtained by calibrating each of the models to 6-month call options on the underlying security in a low-volatility environment. The call option strikes ranged from \$60 to \$140. The low-volatility regime was characterized by a relatively flat skew and an at-the-money (ATM) volatility of approximately 20%. The second

[8]This observation is based on results from an earlier version of this paper where we fitted the normal-BVE distribution using a more complex optimization procedure. In this version of the paper we are using a simple moment-matching approach to fit the distribution. While the numerical results aren't quite as good, moment matching is easy to describe and a commonly employed approximation scheme.

[9]In section 8 we will propose the saddlepoint approximation approach of Glasserman and Kim [10] for pricing LETF options under general AJD dynamics. Even then it is clear from [10] that it would be necessary to tailor the details of the saddlepoint approximation to the specific model dynamics under consideration.

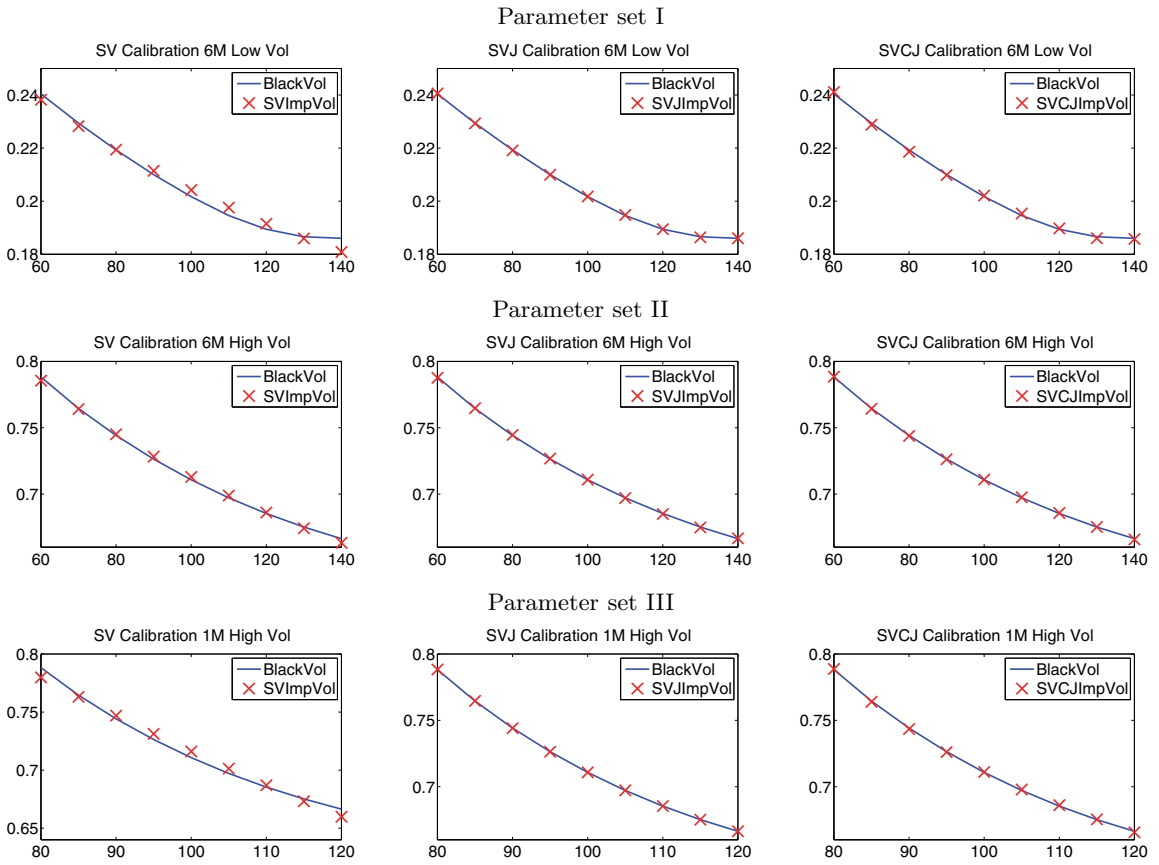

Figure 1. *Volatility skews for the underlying ETF.*

parameter set was obtained by calibrating the three models to 6-month call options on the underlying security in a high-volatility environment with a steeper skew and an ATM volatility of approximately 72%. This high-volatility environment was typical of the environment that prevailed at the height of the financial crisis of 2008. The third parameter set was obtained by calibrating each of the models to 1-month call option prices in the same high-volatility environment that we used for the second parameter set. These environments are reflected by the volatility skews,[10] displayed as blue curves in Figure 1, where we also assumed the underlying price S_0 was \$100. To be clear, the three environments were not obtained from any real market data and therefore constitute an artificially created data-set. Nonetheless it is clear from Figure 1 that these environments are representative of what might be seen in practice.

In each of our models we assumed $r = 0.01$ and $q = f = 0$. With the exception of ρ, the remaining model parameters in each model were calibrated by minimizing the sum-of-squares

[10]We did not have a formal mathematical rule for creating these skews but instead used simple rules of thumb that applied in the marketplace at that time. For example, the implied volatility of a 20-delta option might be 4 to 6 points higher than the implied volatility of the corresponding ATM option.

between the Black–Scholes implied volatilities in the given environment and the Black–Scholes volatilities implied by the model. The parameter ρ was fixed in advance as is commonly the case when calibrating Heston-style models. The reason for this is that it is well known that the sum-of-squares objective function tends to have so-called valleys or directions along which the objective function changes very little. This tends to create a problem for optimization routines, and for this reason it is common to fix ρ in advance to some sensible value.

The Heston model: We set $\rho = -0.76$. The remaining parameters, $(\kappa, \gamma, V_0 = \theta)$, were obtained by minimizing the sum-of-squares as described above.

The SVJ model: We set $\rho = -0.76$ and then solved for the remaining six parameters, $(\kappa, \gamma, V_0 = \theta, \lambda, m, b)$.

The SVCJ model: We set $\rho = -0.82$ and then solved for the remaining eight parameters, $(\kappa, \gamma, V_0 = \theta, \lambda, m, b, \mu_v, \rho_J)$.

The value of ρ for the SV and SVJ models was taken from Broadie and Jain [5], while the value for the SVCJ model was taken from Duffie, Pan, and Singleton [8]. Table 1 displays the calibrated parameters for each of the models in the three environments, and Figure 1 shows that all three models were calibrated successfully to the given implied volatilities[11] in each of the three environments. (The SV model doesn't calibrate quite as well, but this is to be expected given that it has fewer parameters than the SVJ and SVCJ models.)

It is worth mentioning that we calibrated these models only to the prices of options written on the underlying index. An alternative and equally valid (though more difficult) approach would be to try and calibrate simultaneously to index *and* LETF option prices. We chose the former approach for several reasons. First, options on the underlying ETF are more liquid than the corresponding LETF option prices, and so it made sense to focus our calibration effort on these prices. Second, one of the questions we are interested in addressing in this paper is how LETF option prices varied across models. It was much easier to approach this problem by calibrating all models to index option prices only. If the goal is to treat options on the underlying index and LETF equally, then it may be preferable to calibrate to both option types. This would certainly be possible, but given the difficulty of pricing LETF options it would be considerably more time-consuming.

7. Numerical results.

In this section we compute LETF option prices by applying the Carr–Madan transform approach to the characteristic function of the log-LETF price (or approximate log-LETF price in the case of the SVCJ model). We will compare these approximate prices with the assumed exact prices obtained via Monte Carlo. The advantage of the transform approach is that it is much faster than Monte Carlo simulation and allows for the consistent price calculation and risk management of ETF and LETF options in almost real time.

The Monte Carlo prices were obtained using the scheme of Andersen [1], which was designed to simulate the Heston model accurately. In the case of the SVJ and SVCJ models, we simply adapted Andersen to account for the independent jump processes. We assumed a time increment of $\Delta = 0.001$ which, assuming 250 trading days per year, corresponds to an interval of a quarter-day. Within the Monte Carlo simulation we assumed the LETF was

[11] The implied volatilities are computed from the synthetic skews that we defined to model the various environments. These skews are displayed as blue curves in Figure 1.

Table 1
Model parameters.

Parameter set I (calibrated to 6-month option prices in the low-volatility environment).

Parameters	SV model	SVJ model	SVCJ model
Risk free rate r	0.01	0.01	0.01
Speed of mean reversion κ	10.95	0.5012	0.6097
Volatility of variance γ	0.2528	0.0895	0.0776
Long run mean variance θ	0.0421	0.0353	0.0393
Initial variance V_0	0.0421	0.0353	0.0393
Correlation ρ	-0.7571	-0.7571	-0.82
Jump arrival rate λ	n/a	1.0808	0.1406
m	n/a	-0.01	-0.0128
b	n/a	0.0745	0.1152
μ_v	n/a	n/a	0.01
ρ_J	n/a	n/a	0.0013

Parameter set II (calibrated to 6-month option prices in the high volatility environment).

Parameters	SV model	SVJ model	SVCJ model
Risk free rate r	0.01	0.01	0.01
Speed of mean reversion κ	4.9498	0.6500	0.6500
Volatility of variance γ	1.1478	0.7895	0.3377
Long run mean variance θ	0.5505	0.3969	0.4048
Initial variance V_0	0.5505	0.3969	0.4048
Correlation ρ	-0.7571	-0.7571	-0.82
Jump arrival rate λ	n/a	2.1895	0.4996
m	n/a	-0.0105	-0.2592
b	n/a	0.2719	0.4588
μ_v	n/a	n/a	0.094
ρ_J	n/a	n/a	-0.2713

Parameter set III (calibrated to 1-month option prices in the high volatility environment).

Parameters	SV model	SVJ model	SVCJ model
Risk free rate r	0.01	0.01	0.01
Speed of mean reversion κ	10.95	0.3632	0.5474
Volatility of variance γ	1.5086	0.6113	0.5730
Long run mean variance θ	0.5295	0.4156	0.4521
Initial variance V_0	0.5295	0.4156	0.4521
Correlation ρ	-0.7571	-0.7571	-0.82
Jump arrival rate λ	n/a	1.7483	0.5623
m	n/a	-0.1286	-0.2635
b	n/a	0.2384	0.3148
μ_v	n/a	n/a	0.0371
ρ_J	n/a	n/a	0.01

rebalanced every 4 periods, which is equivalent to the daily rebalancing that is performed in practice. Our first task is to compute option prices on the underlying ETF using Carr and Madan's transform approach and Andersen's Monte Carlo scheme. Note that options on the underlying can be priced exactly using the transform approach as the characteristic function

Table 2

Option prices on underlying index/ETF for parameter set II computed via Monte Carlo and transform inversion approaches. Approximate 95% confidence intervals are reported in brackets.

Moneyness	BS vol (%)	BS price	Option price (SV)		Option price (SVJ)		Option price (SVCJ)	
$\frac{K}{S_0}$	Σ_{BS}	C_{BS}	C_{sim}	C_{tran}	C_{sim}	C_{tran}	C_{sim}	C_{tran}
0.75	75.44	33.66	33.66	33.66	33.66	33.66	33.65	33.65
			[33.65, 33.66]	-	[33.65, 33.67]	-	[33.65, 33.66]	
1	71.08	20.04	20.10	20.10	20.05	20.05	20.06	20.05
			[20.09, 20.11]	-	[20.04, 20.06]	-	[20.05, 20.06]	-
1.25	68.03	11.24	11.23	11.23	11.23	11.22	11.25	11.24
			[11.23, 11.24]	-	[11.22, 11.23]	-	[11.24, 11.25]	-

Table 3

Option prices on underlying index/ETF for parameter set III computed via Monte Carlo and transform inversion approaches. Approximate 95% confidence intervals are reported in brackets.

Moneyness	BS vol(%)	BS price	Option price (SV)		Option price (SVJ)		Option price (SVCJ)	
$\frac{K}{S_0}$	Σ_{BS}	C_{BS}	C_{sim}	C_{tran}	C_{sim}	C_{tran}	C_{sim}	C_{tran}
0.9	74.42	13.98	14.01	14.01	13.98	13.98	13.97	13.98
			[14.01, 14.01]	-	[13.98, 13.99]	-	[13.97, 13.98]	
1	71.08	8.04	8.10	8.10	8.05	8.04	8.05	8.05
			[8.10, 8.10]	-	[8.04, 8.05]	-	[8.04, 8.05]	-
1.1	68.54	4.09	4.10	4.10	4.09	4.09	4.10	4.10
			[4.10, 4.11]	-	[4.09, 4.09]	-	[4.09, 4.10]	-

of the log-ETF price is available in this case for all three models. The reason we compute option prices on the underlying ETF is simply to check that the two sets of prices agree modulo statistical error from the simulation and numerical inversion error from the Carr–Madan scheme.

Tables 2 and 3 display these ETF option prices for our three models under parameter sets II and III, respectively. (All of our results for parameter set I, which corresponds to the low-volatility 6-month environment, are deferred to Appendix C.) The Monte Carlo results were based on simulating 10^8 sample paths, which took[12] several hours to run. We required this many paths to get sufficiently narrow confidence intervals so as to allow a comparison of the Monte Carlo prices with the transform prices. It is clear from Tables 2 and 3 that both methods produce ETF option prices that effectively coincide with one another. Given this agreement we are now in a position to consider how well our pricing of LETF options actually performs, particularly[13] in the case of the SVJ and SVCJ models.

In Tables 4 and 5 we display prices of LETF options for parameter sets II and III, respectively, for each of our three models and various leverage ratios. (Recall that obtaining the

[12] All of our numerical experiments were implemented in MATLAB version 7.12.0 (R2011a) on a Windows 7 machine with a 2.53 GHz processor and 4GB of RAM.

[13] Recall that we needed to precompute numerically the characteristic function of the truncated jump component of the log-LETF price for the SVJ model, and that we needed to approximate its distribution for the SVCJ model.

Table 4

Comparing leveraged ETFs option prices with approximate prices in parameter set II. Approximate 95% confidence intervals are reported in brackets.

Leverage ratio	Moneyness		Option price (SV)		Option price (SVJ)		Option price (SVCJ)	
ϕ	$\frac{K_S}{S_0}$	$\frac{K_L}{L_0}$	C_{sim}	C_{tran}	C_{sim}	C_{tran}	C_{sim}	C_{tran}
2	0.75	0.5	60.74	60.66	61.51	61.44	61.66	61.61
			[60.72, 60.76]	-	[61.49, 61.53]	-	[61.64, 61.68]	-
	1	1	37.87	37.78	38.43	38.37	38.50	38.48
			[37.86, 37.89]	-	[38.41, 38.45]	-	[38.48, 38.51]	-
	1.25	1.5	24.18	24.11	24.45	24.41	24.66	24.70
			[24.16, 24.19]	-	[24.43, 24.46]	-	[24.65, 24.68]	-
3	0.75	0.25	81.98	81.82	83.25	83.06	82.39	82.27
			[81.94, 82.01]	-	[83.21, 83.29]	-	[82.35, 82.43]	-
	1	1	53.09	52.77	54.07	53.87	52.93	52.81
			[53.05, 53.12]	-	[54.03, 54.11]	-	[52.90, 52.97]	-
	1.25	1.75	37.60	37.30	37.84	37.69	37.33	37.29
			[37.57, 37.63]	-	[37.80, 37.87]	-	[37.30, 37.36]	-
−1	0.75	1.25	14.15	14.14	13.93	13.90	12.63	13.03
			[14.14, 14.16]	-	[13.92, 13.94]	-	[12.62, 12.64]	-
	1	1	21.19	21.15	21.16	21.10	20.00	20.36
			[21.18, 21.20]	-	[21.15, 21.17]	-	[19.99, 20.01]	-
	1.25	0.75	32.79	32.73	33.24	33.16	32.25	32.51
			[32.78, 32.80]	-	[33.23, 33.25]	-	[32.24, 32.26]	-
−2	0.75	1.5	32.09	31.88	31.29	31.01	27.94	27.94
			[32.05, 32.14]	-	[31.24, 31.33]	-	[27.91, 27.97]	-
	1	1	41.95	41.68	41.60	41.26	38.81	38.75
			[41.90, 41.99]	-	[41.56, 41.64]	-	[38.78, 38.84]	-
	1.25	0.5	60.25	60.02	61.09	60.76	59.08	59.01
			[60.21, 60.30]	-	[61.04, 61.13]	-	[59.05, 59.11]	-
−3	0.75	1.75	51.48	50.72	49.43	48.46	44.41	43.96
			[51.19, 51.77]	-	[49.18, 49.69]	-	[44.31, 44.51]	-
	1	1	60.88	60.17	59.56	58.59	55.77	55.30
			[60.59, 61.18]	-	[59.31, 59.82]	-	[55.67, 55.87]	-
	1.25	0.25	81.74	81.46	82.59	81.89	80.65	80.44
			[81.45, 82.04]	-	[82.33, 82.85]	-	[80.55, 80.76]	-

Monte Carlo prices took several hours, so the discussion here refers only to the prices C_{tran} obtained via numerical transform inversion.) The most computationally demanding task was pricing the LETF options under the SVJ model: for each parameter set and each leverage ratio, it took about one minute to obtain the three option prices. Almost all of this time was spent computing the characteristic function of the log-truncated jump distribution on a grid of 10,000 points. Given the accuracy of the prices we obtained, we could easily have improved the run-time of these calculations by using a coarser grid of points. Moreover, we could have used instead the moment-matching approach that we adopted for the SVCJ model. While not quite as accurate, this latter approach only took approximately one-tenth of a second to perform the moment matching for a given leverage ratio and then price the three options corresponding to that ratio. Pricing the LETF options for the SV model took even less time

Table 5

Comparing leveraged ETFs option prices with approximate prices in parameter set III. Approximate 95% confidence intervals are reported in brackets.

Leverage ratio	Moneyness		Option price (SV)		Option price (SVJ)		Option price (SVCJ)	
ϕ	$\frac{K_S}{S_0}$	$\frac{K_L}{L_0}$	C_{sim}	C_{tran}	C_{sim}	C_{tran}	C_{sim}	C_{tran}
2	0.9	0.8	27.10	27.03	27.32	27.28	27.18	27.13
			[27.10, 27.11]	-	[27.32, 27.33]	-	[27.17, 27.19]	-
	1	1	15.98	15.94	16.06	16.04	15.97	15.94
			[15.98, 15.99]	-	[16.05, 16.06]	-	[15.96, 15.97]	-
	1.1	1.2	8.66	8.66	8.75	8.76	8.71	8.72
			[8.66, 8.67]	-	[8.74, 8.75]	-	[8.70, 8.71]	-
3	0.9	0.7	39.31	39.09	39.70	39.56	39.22	39.08
			[39.30, 39.32]	-	[39.69, 39.71]	-	[39.21, 39.23]	-
	1	1	23.65	23.49	23.78	23.70	23.45	23.38
			[23.65, 23.66]	-	[23.77, 23.79]	-	[23.44, 23.46]	-
	1.1	1.3	13.64	13.58	13.74	13.76	13.56	13.59
			[13.63, 13.65]	-	[13.74, 13.75]	-	[13.56, 13.57]	-
−1	0.9	1.1	4.81	4.84	4.54	4.55	4.57	4.51
			[4.81, 4.81]	-	[4.53, 4.54]	-	[4.57, 4.58]	-
	1	1	8.25	8.24	8.02	8.00	8.05	7.97
			[8.25, 8.25]	-	[8.02, 8.02]	-	[8.05, 8.06]	-
	1.1	0.9	13.58	13.53	13.48	13.44	13.50	13.40
			[13.57, 13.58]	-	[13.48, 13.49]	-	[13.49, 13.50]	-
−2	0.9	1.2	10.39	10.41	9.61	9.61	9.72	9.75
			[10.39, 10.40]	-	[9.60, 9.61]	-	[9.72, 9.73]	-
	1	1	16.58	16.49	15.96	15.86	16.06	15.98
			[16.58, 16.59]	-	[15.95, 15.97]	-	[16.05, 16.06]	-
	1.1	0.8	26.49	26.32	26.24	26.07	26.26	26.11
			[26.48, 26.50]	-	[26.23, 26.25]	-	[26.26, 26.27]	-
−3	0.9	1.3	16.72	16.61	15.19	15.11	15.44	15.33
			[16.71, 16.73]	-	[15.18, 15.20]	-	[15.43, 15.45]	-
	1	1	25.02	24.70	23.81	23.54	24.02	23.72
			[25.00, 25.03]	-	[23.80, 23.82]	-	[24.01, 24.03]	-
	1.1	0.7	38.74	38.31	38.23	37.87	38.31	37.91
			[38.73, 38.76]	-	[38.22, 38.25]	-	[38.30, 38.32]	-

as no approximations were required.

Figures 2 and 3 display an alternative view of the results in Tables 4 and 5, respectively. Each figure consists of five subplots, one for each value of the leverage ratio, ϕ. These subplots show the percentage relative pricing error for each of the three models. We take the daily rebalanced Monte Carlo price as the "true" price and the transform-inversion price as the "approximate" price.

Before analyzing the results, we first consider the possible sources of discrepancy between the reported Monte Carlo prices and the prices obtained via numerical transform inversion. There are four such sources:

(i) Our Monte Carlo assumed that the leveraged ETFs were rebalanced at a daily frequency as is the case in practice. The transform approach, however, implicitly assumes

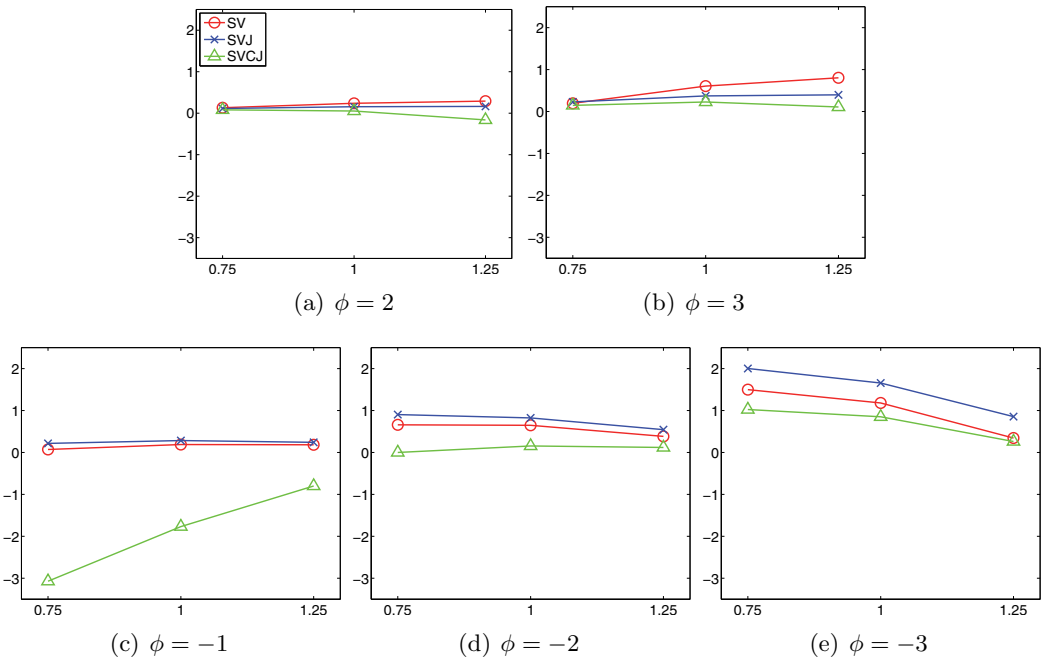

Figure 2. *Percentage relative error,* $\frac{(C_{sim}-C_{tran})}{C_{tran}} \times 100$*, of approximate LETF option prices for parameter set II.*

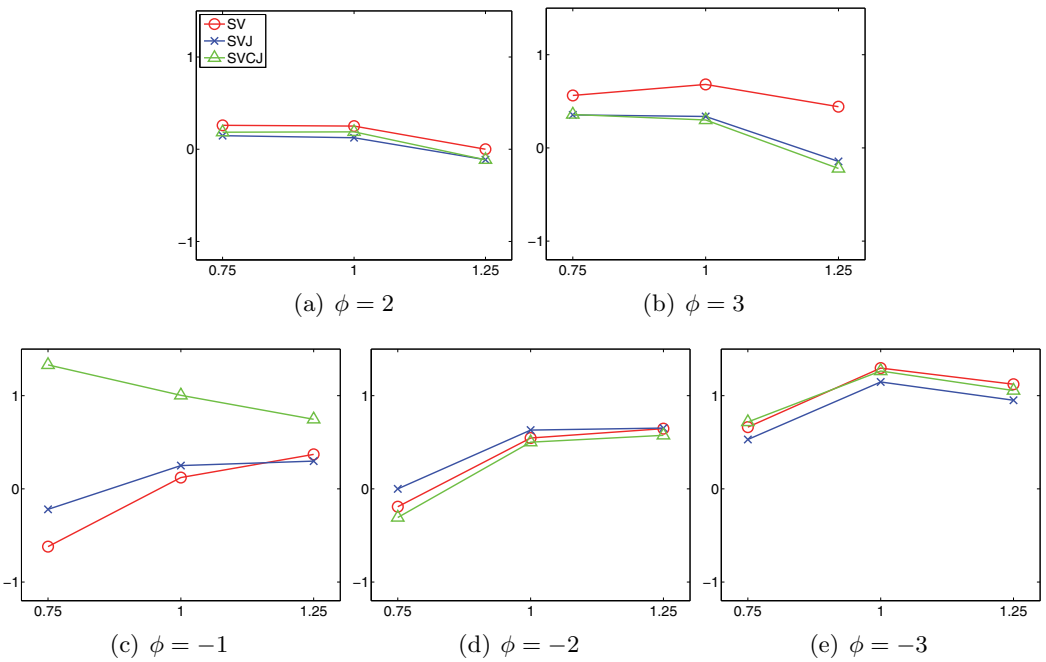

Figure 3. *Percentage relative error,* $\frac{(C_{sim}-C_{tran})}{C_{tran}} \times 100$*, of approximate LETF option prices for parameter set III.*

that the rebalancing takes place continuously. We will see in Table 6 below that this is a principal source of the discrepancy between the Monte Carlo prices and the approximate prices.

(ii) Numerical transform inversion is also a source of error, but we believe this error to be very small and on the order of at most 1 or 2 cents. This claim is justified in part by the results in Tables 2 and 3.

(iii) Statistical error in the reported Monte Carlo prices. We ensured this error was small by simulating sufficiently many paths so as to ensure that the approximate 95% confidence intervals were just 1 or 2 cents wide.

(iv) The fourth source are the errors that arise from (i) the numerical precomputation of the characteristic function of the truncated jump component of the log-LETF price in the case of the SVJ model, and (ii) our approximation of the jump size distribution in the case of the SVCJ model.

The main observation from Tables 4 and 5 (and Figures 2 and 3) is that the approximate LETF option prices as reported in the C_{tran} columns are very close to the reported Monte Carlo prices. The most noticeable discrepancy occurs for some options with leverage ratios of -3 in Table 4, where the discrepancy between the simulation and transform-based prices is sometimes on the order of 1% or 2%. But in a high-volatility environment these errors should easily fall within the bid-ask spreads found in practice. We note that the errors are much smaller for the 3-month high-volatility environment options of Table 5 and are practically nonexistent for the low-volatility environment of Table 15 corresponding to parameter set 1.

We also note that the Monte Carlo prices are generally higher than the transform-based prices. This is presumably due to the fact that prices computed via the transform approach are based on continuous rebalancing of the LETFs, whereas the Monte Carlo prices are computed assuming the LETF is rebalanced daily. This is also suggested by the prices in the SV model where LETF option pricing is exact (modulo transform inversion error) but where we still see a discrepancy between Monte Carlo and transform prices that is comparable to the discrepancies we observe in the SVJ and SVCJ models.

We can confirm this observation by examining the option prices in Table 6, where we also report Monte Carlo prices that were estimated assuming the LETF was rebalanced 4 times per day rather than just once per day. In that table we see that the Monte Carlo prices based on rebalancing four times per day are generally much closer to the transform-based prices. Presumably if we were to increase the LETF rebalancing frequency, then the Monte Carlo and transform-based prices would be in even closer agreement. These observations justify our earlier observation that most of the discrepancy in Tables 4 and 5 between the Monte Carlo prices and transform-based prices is due to the differences in rebalancing frequency.

Another observation regarding Table 6 is that, with the exception of the SVCJ model, LETF option prices appear to be monotonic with respect to rebalancing frequency for a given leverage ratio and moneyness value. In particular, we see that $C_{sim}^{(1)} \geq C_{sim}^{(4)} \geq C_{tran}$ is generally satisfied for the SV and SVJ models. (Recall our earlier observation that C_{tran} corresponds to a continuous rebalancing assumption.) In the case of the SVCJ model we do observe that $C_{sim}^{(1)} \geq C_{sim}^{(4)}$ but the pattern is broken with C_{tran}. This is likely due to the fact that C_{tran} is computed using approximate LETF dynamics, whereas the Monte Carlo prices

Table 6

Comparison of LETF option prices obtained by Monte Carlo simulation with different rebalancing frequencies in parameter set II. $C_{sim}^{(1)}$ corresponds to daily rebalancing, and $C_{sim}^{(4)}$ corresponds to rebalancing 4 times per day. C_{tran} refers to prices that were obtained via numerical transform inversion.

Leverage ratio	Moneyness		Option price (SV)			Option price (SVJ)			Option price (SVCJ)		
ϕ	$\frac{K_S}{S_0}$	$\frac{K_L}{L_0}$	$C_{sim}^{(1)}$	$C_{sim}^{(4)}$	C_{tran}	$C_{sim}^{(1)}$	$C_{sim}^{(4)}$	C_{tran}	$C_{sim}^{(1)}$	$C_{sim}^{(4)}$	C_{tran}
2	0.75	0.5	60.74	60.69	60.66	61.51	61.46	61.44	61.66	61.61	61.61
	1	1	37.87	37.81	37.78	38.43	38.39	38.37	38.50	38.46	38.48
	1.25	1.5	24.18	24.13	24.11	24.45	24.42	24.41	24.66	24.65	24.70
3	0.75	0.25	81.98	81.88	81.82	83.25	83.12	83.06	82.39	82.28	82.27
	1	1	53.09	52.87	52.77	54.07	53.92	53.87	52.93	52.80	52.81
	1.25	1.75	37.60	37.39	37.30	37.84	37.73	37.69	37.33	37.24	37.29
−1	0.75	1.25	14.15	14.14	14.14	13.93	13.90	13.90	12.63	12.62	13.03
	1	1	21.19	21.16	21.15	21.16	21.12	21.10	20.00	19.97	20.36
	1.25	0.75	32.79	32.74	32.73	33.24	33.18	33.16	32.25	32.21	32.51
−2	0.75	1.5	32.09	31.93	31.88	31.29	31.06	31.01	27.94	27.81	27.94
	1	1	41.95	41.74	41.68	41.60	41.33	41.26	38.81	38.65	38.75
	1.25	0.5	60.25	60.08	60.02	61.09	60.83	60.76	59.08	58.95	59.01
−3	0.75	1.75	51.48	50.80	50.72	49.43	48.59	48.46	44.41	43.99	43.96
	1	1	60.88	60.24	60.17	59.56	58.72	58.59	55.77	55.36	55.30
	1.25	0.25	81.74	81.43	81.46	82.59	81.96	81.89	80.65	80.48	80.44

are computed using the true LETF dynamics.

A final observation from Tables 4 and 5 is that there is some discrepancy in LETF option prices across the three different models. For example, in Table 4 we see that with $\phi = -3$ and $K_L/L_0 = 1.75$ the LETF call option price is approximately \$51, \$49, and \$44 under the SV, SVJ, and SVCJ models, respectively. This is despite the fact that all three models were calibrated to the same 6-month implied volatilities. Of course, this observation is not too surprising as the LETF price is path dependent, and so it is not the case that the 6-month LETF option prices will only depend on the risk-neutral distribution of S_t where $t = 6$ months. This difference in LETF option prices across models is less noticeable in the 1-month options of parameter set III in Table 5. It is also worth pointing out that the 6-month LETF option prices vary very little by model in the low-volatility environment of parameter set I. These prices are displayed in Appendix C. We will return to this issue in section 7.1.

7.1. Comparing the LETF implied volatilities across different models. We now report the LETF option prices in terms of their Black-Scholes implied volatilities. We have already seen that there is some variability in these prices across the different models, but it would be interesting to see this variability expressed in units of implied volatility. This will also allow us to consider the commonly used practice of computing an LETF option price via the Black–Scholes formula with the implied volatility taken (and scaled appropriately) from a corresponding underlying index (or ETF) option price. We will also introduce an additional model, namely, the Barndorff-Nielsen and Shephard (BNS) model (see [3]), as this model helps to provide an even clearer demonstration of the fact that LETF option prices are strongly path dependent and are not uniquely determined by the implied volatility surface of the underlying

index or ETF. In particular, we will see that introducing the BNS model into our set of model will broaden (and sometimes dramatically) the range of plausible LETF option prices. We first describe the BNS model.

The BNS model. The variance process is modeled by an Ornstein–Uhlenbeck (OU) process driven by a Levy process with nonnegative increments. In particular we will assume that the variance process is a gamma-OU process and that the risk-neutral dynamics for the security price and instantaneous variance are

$$d\log S_t = \left(r - q - \frac{a\lambda\rho}{b-\rho} - \frac{V_t}{2}\right)dt + \sqrt{V_t}dW_t + \rho dz_{\lambda\cdot t},$$
$$dV_t = -\lambda V_t dt + dz_{\lambda\cdot t},$$

where W_t is a standard Brownian motion and z_t is a compound Poisson process with $z_t = \sum_{n=1}^{N_t} x_n$, where the Poisson process N_t has intensity a and the x_i's are independent and identically distributed exponential random variables with mean $1/b$. We also assume $\lambda > 0$ and $V_0 > 0$ so that (since $dz_{\lambda\cdot t}$ is always nonnegative) $\inf_{0\le t\le T} V_t \ge \exp(-\lambda T) > 0$. The parameter ρ is typically negative to account for the negative correlation between variance and the underlying price process. Note that the variance can only jump upward and that between jumps it decays exponentially. With a negative value of ρ the security price will jump downward when a jump in variance occurs, and it is worth noting in this case that leveraged ETFs with $\phi < 0$ can then only jump upward in price. There is therefore no need to truncate the jumps of the LETF price process in this case, and indeed the LETF price process will itself have BNS dynamics. When $\phi > 0$ this will not be true as it will be necessary to truncate the jumps of the underlying ETF. In this case we could try to approximate the jump process as we did with the SVJ and SVCJ models and then obtain approximate LETF option prices using transform methods. Rather than doing this, however, we will simply price the LETF options using Monte Carlo because our goal in this section is to simply investigate how model dependent LETF option prices are.

We calibrated the BNS model to the same implied volatility skews of Figure 1 and note here that this calibration was performed successfully so that all four models agreed on the prices of options on the underlying ETF. This agreement can be seen in Tables 10 and 11 in Appendix A by noting that the columns labeled Σ_S are practically identical across the four models. The prices of the LETF options across the four models and various leverage ratios are displayed in Table 7. The same results, except in terms of implied volatilities, are displayed in Tables 10 and 11 (and Figures 4 and 5) for parameter sets II and III, respectively. The LETF option implied volatilities are displayed in the columns labeled Σ_L and are calculated using the LETF option prices from Tables 4 and 5.

In order to compute the implied volatility ratios, $\frac{\Sigma_L}{\Sigma_S}$, we aligned[14] the options on the underlying ETF and the leveraged ETF on a "strike-equivalent basis" to account for the leverage. For example, we align a 25% out-of-the-money option on the underlying ETF with

[14]We also note that Leung and Sircar [16] proposed an alternative approach for aligning or comparing options on the underlying with options on the LETF. Their approach is to compute the implied volatility of the LETF options and then divide them by the (absolute) value of the leverage ratio. This approach seems more appropriate for their goal, namely, studying how the underlying skew influences the LETF skew.

Table 7

Comparison for the prices of options on the leveraged ETFs obtained by Monte Carlo simulation in parameter sets II and III.

Leverage ratio	Moneyness		Parameter set II				Moneyness		Parameter set III			
ϕ	$\frac{K_S}{S_0}$	$\frac{K_L}{L_0}$	C_{sim}^{SV}	C_{sim}^{SVJ}	C_{sim}^{SVCJ}	C_{sim}^{BNS}	$\frac{K_S}{S_0}$	$\frac{K_L}{L_0}$	C_{sim}^{SV}	C_{sim}^{SVJ}	C_{sim}^{SVCJ}	C_{sim}^{BNS}
2	0.75	0.5	60.74	61.51	61.66	63.20	0.9	0.8	27.10	27.32	27.18	27.50
	1	1	37.87	38.43	38.50	40.55	1	1	15.98	16.06	15.97	16.26
	1.25	1.5	24.18	24.45	24.66	26.64	1.1	1.2	8.66	8.75	8.71	8.93
3	0.75	0.25	81.98	83.25	82.39	85.18	0.9	0.7	39.31	39.70	39.22	40.50
	1	1	53.09	54.07	52.93	57.81	1	1	23.65	23.78	23.45	24.62
	1.25	1.75	37.60	37.84	37.33	42.29	1.1	1.3	13.64	13.74	13.56	14.47
−1	0.75	1.25	14.15	13.93	12.63	11.53	0.9	1.1	4.81	4.54	4.57	4.39
	1	1	21.19	21.16	20.00	18.92	1	1	8.25	8.02	8.05	7.86
	1.25	0.75	32.79	33.24	33.25	31.48	1.1	0.9	13.58	13.48	13.50	13.35
−2	0.75	1.5	32.09	31.29	27.94	24.88	0.9	1.2	10.39	9.61	9.72	9.18
	1	1	41.95	41.60	38.81	36.15	1	1	16.58	15.96	16.06	15.50
	1.25	0.5	60.25	61.09	59.08	57.72	1.1	0.8	26.49	26.24	26.26	25.88
−3	0.75	1.75	51.48	49.43	44.41	39.00	0.9	1.3	16.72	15.19	15.44	14.36
	1	1	60.88	59.56	55.77	51.48	1	1	25.02	23.81	24.02	22.97
	1.25	0.25	81.74	82.59	80.65	79.48	1.1	0.7	38.74	38.23	38.31	37.64

a 50% out-of-the-money option on a double-long LETF to account for the higher leverage of $\phi = 2$. We note that the implied volatility ratio tends to be close to the leverage ratio, ϕ, but that there can be a considerable discrepancy between the two. The degree of this discrepancy is model dependent and is very notable for the BNS model (which is why we have included the BNS model here). For a given model, it is also the case that whether or not the ratio $\frac{\Sigma_L}{\Sigma_S}$ is greater than ϕ depends on whether or not the LETF is positively or negatively leveraged. We emphasize again here that these observations are based on parameter set II, which models the 6-month, high-volatility environment.

8. Saddlepoint approximations. The affine jump-diffusion (AJD) models of Duffie, Pan, and Singleton [8] are a rich and flexible class under which the prices of many derivative security types can be obtained via the numerical inversion of extended transforms. In general, however, these extended transforms can only be computed numerically as the solution of a series of ODEs. In order to compute derivative security prices it is therefore necessary (in general) to solve a series of ODEs for each integration point in the aforementioned numerical transform inversion. This has limited application of AJD models in practice to the much smaller subset of models for which the transforms are available in closed form. We note that even though the SVJ and SVCJ models considered in this paper are AJD models where the transforms are known in closed form, this is not true for the LETF dynamics in those models: truncating the jumps results in AJD models where the transforms are not available in closed form.

Glasserman and Kim [11] proposed the use of saddlepoint approximations to tackle this issue. More specifically, it is well known that the calculation of option prices can be reduced to the calculation of tail probabilities of the form $Q(Y > y)$, where $Y = \log(S_T)$, the log-security price at time T, and Q is an equivalent martingale measure corresponding to some given

numeraire. In the AJD setting this tail probability can be calculated via Fourier inversion according to

$$Q(Y > y) = \frac{1}{2\pi i} \int_{\tau - i\infty}^{\tau + i\infty} e^{(\mathcal{K}(z) - zy)} \frac{dz}{z}, \quad \tau > 0, \tag{8.1}$$

where $\mathcal{K}$ is the cumulant-generating function (CGF) of the log-security price, i.e., $e^{\mathcal{K}(z)} = \mathbb{E}(e^{z \log(S_T)})$. We can therefore price options by performing a numerical integration to compute the right-hand side of (8.1). Unfortunately, for each evaluation point z in the numerical integration, we must in general solve a series of ODEs to compute $\mathcal{K}(z)$. As mentioned above, this seriously limits the applicability of AJD models to those models where $\mathcal{K}(z)$ is available in closed form.

Glasserman and Kim's contribution was to recognize that if $\mathcal{K}(z)$ is not available in closed form, then it would still be possible to obtain an accurate approximation to (8.1) using a saddlepoint approximation. Their approximation requires the calculation of $\mathcal{K}(\hat{z})$ as well as the first and second derivatives, $\mathcal{K}'(\hat{z})$ and $\mathcal{K}''(\hat{z})$, at the saddlepoint, $\hat{z}$. The saddlepoint satisfies $\mathcal{K}'(\hat{z}) = y$, and most of the computational work is expended in solving[15] this equation. (Calculation of $\mathcal{K}(\hat{z})$, $\mathcal{K}'(\hat{z})$, and $\mathcal{K}''(\hat{z})$ requires solving three systems of ODEs. This is a significant improvement over having to solve a system of ODEs for each integration point z.) In their numerical experiments, Glasserman and Kim obtain accurate option prices via their saddlepoint approximations, but they also find that no one approach dominates. While their LR approximation provides the best overall performance, they recommend[16] tailoring the specific approximation to the level of moneyness and time-to-maturity.

In order to examine the performance of the saddlepoint technique for pricing LETF options, we applied[17] it to the SV model under the high-volatility parameter sets II and III. In Tables 8 and 9 we compare the LETF option prices that were obtained using three different methods: Monte Carlo, numerical transform inversion, and saddlepoint approximation. (Recall that when the underlying index/ETF has SV dynamics, then the LETF also has SV dynamics, and therefore numerical transform inversion yields exact option prices (assuming continuous rebalancing of the LETF).) We see that the transform inversion and saddlepoint prices practically coincide: the price difference is a cent or less in every case. This admittedly limited experiment suggests that the saddlepoint approach is also capable of producing accurate LETF option prices for other AJD price dynamics. Given the observations of Glasserman and Kim, however, it's unlikely that the saddlepoint approach can be used in a black-box fashion for all AJD models. In particular, some tailoring of the approach to each model under consideration would be required.

9. Conclusions.

We have shown how to obtain accurate LETF option prices via transform pricing methods for the Heston (SV) model as well as two related jump-diffusion models, namely, the SVJ and SVCJ models. Our option prices for the SV and SVJ models were

[15] Glasserman and Kim consider several approaches for finding $\hat{z}$, including the Lieberman approximation, the Lugannani–Rice (LR) formula, and variations of the LR formula.

[16] In a similar spirit, we would recommend tailoring jump distribution of the moment-matching approach to the specific AJD model under consideration.

[17] We are grateful to Kyoung-Kuk Kim for providing us with MATLAB code that we could easily adapt to pricing the LETF options in the SV model.

Table 8

Comparing LETF option prices in the SV model under parameter set II. $C_{saddlepoint}$ refers to prices that were obtained via a saddlepoint approximation.

Leverage ratio	Moneyness		Option price		
ϕ	$\frac{K_S}{S_0}$	$\frac{K_L}{L_0}$	C_{sim}	C_{tran}	$C_{saddlepoint}$
2	0.75	0.5	60.74	60.66	60.66
	1	1	37.87	37.78	37.78
	1.25	1.5	24.18	24.11	24.10
3	0.75	0.25	81.98	81.82	81.82
	1	1	53.09	52.77	52.76
	1.25	1.75	37.60	37.30	37.29
−1	0.75	1.25	14.15	14.14	14.14
	1	1	21.19	21.15	21.15
	1.25	0.75	32.79	32.73	32.72
−2	0.75	1.5	32.09	31.88	31.88
	1	1	41.95	41.68	41.67
	1.25	0.5	60.25	60.02	60.01
−3	0.75	1.75	51.48	50.72	50.72
	1	1	60.88	60.17	60.17
	1.25	0.25	81.74	81.46	81.46

Table 9

Comparing LETF option prices in the SV model under parameter set III. $C_{saddlepoint}$ refers to prices that were obtained via a saddlepoint approximation.

Leverage ratio	Moneyness		Option price		
ϕ	$\frac{K_S}{S_0}$	$\frac{K_L}{L_0}$	C_{sim}	C_{tran}	$C_{saddlepoint}$
2	0.9	0.8	27.10	27.03	27.03
	1	1	15.98	15.94	15.94
	1.1	1.2	8.66	8.66	8.66
3	0.9	0.7	39.31	39.09	39.09
	1	1	23.65	23.49	23.49
	1.1	1.3	13.64	13.58	13.59
−1	0.9	1.1	4.81	4.84	4.84
	1	1	8.25	8.24	8.24
	1.1	0.9	13.58	13.53	13.53
−2	0.9	1.2	10.39	10.41	10.41
	1	1	16.58	16.49	16.49
	1.1	0.8	26.49	26.32	26.32
−3	0.9	1.3	16.72	16.61	16.61
	1	1	25.02	24.70	24.70
	1.1	0.7	38.74	38.31	38.31

exact, but in the case of the SVCJ model we proposed approximate price dynamics for the LETF based on approximating its (truncated) jump distribution. We find our methodology works very well in both low- and high-volatility environments, and because they are consistent

with the prices of options on the underlying ETF, they permit consistent pricing and risk-management of derivatives portfolios containing both ETF and LETF options. It should also be clear that similar approximation techniques could be applied to other jump-diffusion models, and so our examples should be viewed as applications of a more general approximation technique. We have also proposed the saddlepoint approximation approach of Glasserman and Kim [10] as an alternative approach which can be used for general affine jump-diffusion price dynamics. Nevertheless, we note that these approximation methods do need to be tailored to the specific model under consideration.

In addition to confirming the accuracy of our LETF option prices, our numerical experiments also showed that the ratio of an LETF option implied volatility to the corresponding ETF option implied volatility can be far from the LETF leverage ratio. This, of course, can also be seen from market prices of options on ETFs and corresponding LETFs. The difference between the two depends on whether or not the LETF is long or short and is model dependent, thereby emphasizing the path dependence of the LETF price at any given time. This calls into question the market practice of pricing an LETF option using the Black–Scholes formula with the strike and implied volatility from the underlying ETF scaled by the leverage ratio. In particular, it should be clear that using the Black–Scholes formula in this manner amounts to the implicit assumption of (generally unspecified) dynamics for the underlying ETF.

Appendix A. Log-price characteristic functions.

The Heston model. The characteristic function of the log-security price under the Heston model is (see [19], for example) given by

$$\begin{aligned}\Phi_T^{SV}(u;r,q,\kappa,\gamma,\theta,V_0,\rho,S_0) &= \exp\left[iu(\log(S_0)+(r-q)T)\right]\\ &\times \exp\left[\theta\kappa\gamma^{-2}\left((\kappa-\rho\gamma ui-d)T-2\log((1-g\exp(-dT))/(1-g))\right)\right]\\ &\times \exp\left[V_0\gamma^{-2}(\kappa-\rho\gamma ui-d)\left(1-\exp(-dT)\right)/\left(1-g\exp(-dT)\right)\right],\end{aligned} \tag{A.1}$$

where $d := \sqrt{(\rho\gamma ui-\kappa)^2+\gamma^2(iu+u^2)}$ and $g := (\kappa-\rho\gamma ui-d)/(\kappa-\rho\gamma ui+d)$.

The Bates model. The characteristic function of the log-security price under the SVJ model is

$$\begin{aligned}\Phi_T^{SVJ}(u;r,q,\kappa,\gamma,\theta,V_0,\rho,S_0,\lambda,a,b) &= \Phi_T^{SV}(u\,;r,q,\kappa,\gamma,\theta,V_0,\rho,S_0)\times\exp(-\lambda miuT)\\ &\times\exp\left[\lambda T\left(\exp\left(aiu-\frac{b^2u^2}{2}\right)-1\right)\right],\end{aligned} \tag{A.2}$$

where $m := \exp\left(a+\frac{b^2}{2}\right)-1$.

The BNS model. The characteristic function of the log-security price under the BNS model is

$$\begin{aligned}\Phi_T^{BNS}(u;r,q,a,b,V_0,\lambda,\rho,S_0) &= \exp\left[iu\left(\log(S_0)+(r-q-a\lambda\rho(b-\rho)^{-1})T\right)\right]\\ &\times\exp\left[-\lambda^{-1}(u^2+ui)(1-\exp(-\lambda T))V_0/2\right]\\ &\times\exp\left[a(b-f_2)^{-1}\left(b\log\left(\frac{b-f_1}{b-ui\rho}\right)+f_2\lambda T\right)\right],\end{aligned} \tag{A.3}$$

Table 10

Comparison of Black–Scholes implied volatilities: Parameter set II.

Leverage ratio	Moneyness		Implied volatility (SV)			Implied volatility (SVJ)			Implied volatility (SVCJ)			Implied volatility (BNS)		
ϕ	$\frac{K_S}{S_0}$	$\frac{K_L}{L_0}$	Σ_S	Σ_L	$\frac{\Sigma_L}{\Sigma_S}$	Σ_S	Σ_L	$\frac{\Sigma_L}{\Sigma_S}$	Σ_S	Σ_L	$\frac{\Sigma_L}{\Sigma_S}$	Σ_S	Σ_L	$\frac{\Sigma_L}{\Sigma_S}$
2	0.75	0.5	75.42	149.10	1.98	75.44	154.61	2.05	75.40	155.73	2.07	75.41	166.68	2.21
	1	1	71.28	139.11	1.95	71.10	141.35	1.99	71.13	141.62	1.99	71.09	149.98	2.11
	1.25	1.5	68.00	133.12	1.96	67.98	134.07	1.97	68.05	134.85	1.98	68.04	141.88	2.09
3	0.75	0.25		224.18	2.97		242.31	3.21		230.05	3.05		270.14	3.58
	1	1		204.20	2.86		208.76	2.94		203.50	2.86		226.66	3.19
	1.25	1.75		195.88	2.88		196.76	2.89		194.89	2.86		213.52	3.14
-1	0.75	1.25		78.48	1.04		77.69	1.03		73.04	0.97		69.07	0.92
	1	1		75.29	1.06		75.20	1.06		70.93	1.00		66.95	0.94
	1.25	0.75		71.11	1.05		73.36	1.08		68.39	1.01		64.44	0.95
-2	0.75	1.5		161.47	2.14		158.55	2.10		146.52	1.94		135.62	1.80
	1	1		155.70	2.18		154.26	2.17		142.90	2.01		132.23	1.86
	1.25	0.5		145.60	2.14		151.60	2.23		137.08	2.01		126.99	1.87
-3	0.75	1.75		250.11	3.32		241.67	3.20		221.67	2.94		201.07	2.67
	1	1		242.04	3.40		235.34	3.31		216.79	3.05		196.86	2.77
	1.25	0.25		220.82	3.25		232.95	3.43		205.07	3.01		187.56	2.76

Table 11

Comparison of Black–Scholes implied volatilities: Parameter set III.

Leverage ratio	Moneyness		Implied volatility (SV)			Implied volatility (SVJ)			Implied volatility (SVCJ)			Implied volatility (BNS)		
ϕ	$\frac{K_S}{S_0}$	$\frac{K_L}{L_0}$	Σ_S	Σ_L	$\frac{\Sigma_L}{\Sigma_S}$	Σ_S	Σ_L	$\frac{\Sigma_L}{\Sigma_S}$	Σ_S	Σ_L	$\frac{\Sigma_L}{\Sigma_S}$	Σ_S	Σ_L	$\frac{\Sigma_L}{\Sigma_S}$
2	0.9	0.8	74.70	149.29	2.00	74.43	151.86	2.04	74.33	150.19	2.02	74.47	153.92	2.07
	1	1	71.59	142.28	1.99	71.09	142.98	2.01	71.10	142.18	2.00	71.09	144.82	2.04
	1.1	1.2	68.68	136.37	1.99	68.55	137.13	2.00	68.61	136.78	1.99	68.57	138.82	2.02
3	0.9	0.7		224.42	3.00		229.50	3.08		223.22	3.00		239.89	3.22
	1	1		212.51	2.97		213.65	3.01		210.62	2.96		221.45	3.12
	1.1	1.3		203.50	2.96		204.42	2.98		202.82	2.96		210.92	3.08
-1	0.9	1.1		75.38	1.01		72.78	0.98		73.14	0.98		71.41	0.96
	1	1		72.90	1.02		70.85	1.00		71.16	1.00		69.40	0.98
	1.1	0.9		70.06	1.02		69.04	1.01		69.18	1.01		67.55	0.99
-2	0.9	1.2		152.14	2.04		145.04	1.95		146.08	1.97		141.10	1.89
	1	1		147.73	2.06		142.09	2.00		142.95	2.01		137.94	1.94
	1.1	0.8		142.13	2.07		139.12	2.03		139.43	2.03		134.80	1.97
-3	0.9	1.3		231.00	3.09		217.39	2.92		219.57	2.95		209.93	2.82
	1	1		225.17	3.15		213.95	3.01		215.89	3.04		206.21	2.90
	1.1	0.7		216.96	3.16		210.24	3.07		211.25	3.08		202.31	2.95

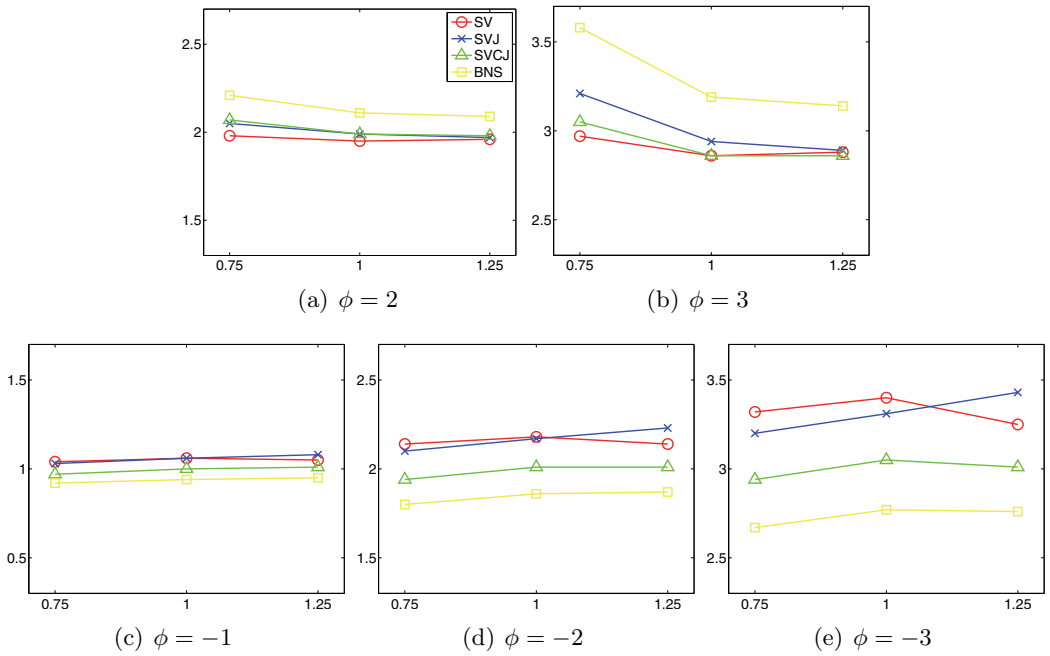

Figure 4. *Ratio of the Black–Scholes implied volatilities for the underlying and leveraged ETF options (rescaled by strike), $\frac{\Sigma_L}{\Sigma_S}$, for parameter set II.*

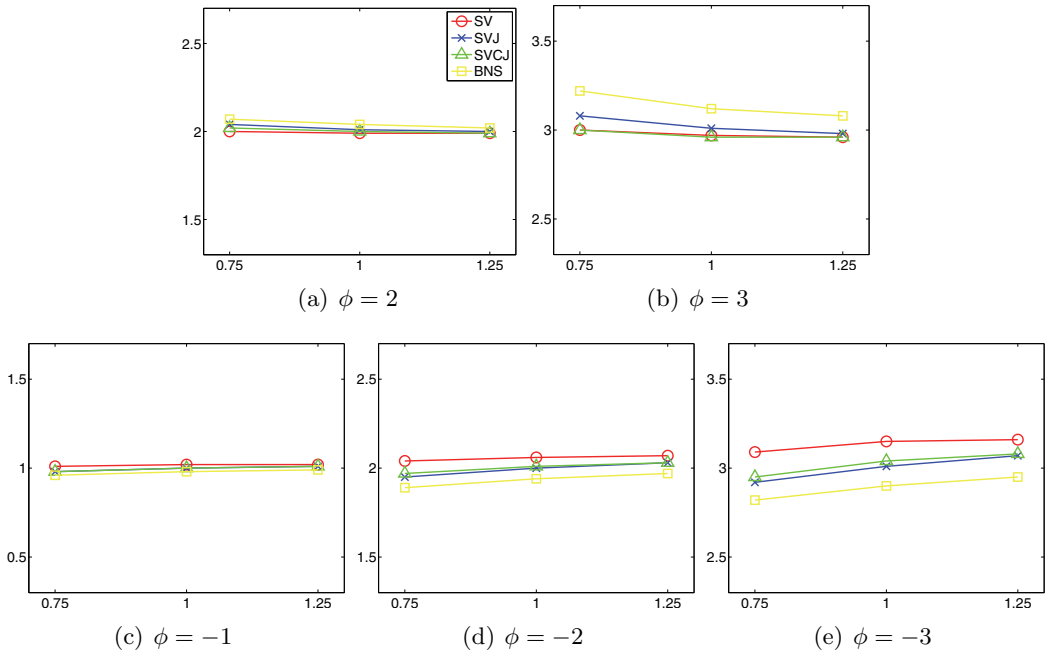

Figure 5. *Ratio of the Black–Scholes implied volatilities for the underlying and leveraged ETF options (rescaled by strike), $\frac{\Sigma_L}{\Sigma_S}$, for parameter set III.*

where

$$f_1 = f_1(u) = ui\rho - \lambda^{-1}(u^2 + ui)(1 - \exp(-\lambda T))/2,$$
$$f_2 = f_2(u) = ui\rho - \lambda^{-1}(u^2 + ui)/2.$$

Appendix B. The SVCJ model. Following Duffie, Pan, and Singleton [8] we can use the SVCJ model to price options on the underlying ETF. Indeed the characteristic function of the log-ETF price under the SVCJ model is given by

(B.1)
$$\Phi_T^{SVCJ}(u; r, q, \kappa, \gamma, \theta, V_0, \rho, S_0, \lambda, a, b, \rho_J, \mu_v) = \exp(A(0,T,u) + iu\log(S_0) + C(0,T,u)V_0),$$

where

$$C(t,T,u) = -\frac{a_1(1 - e^{-a_4\tau})}{2a_4 - (a_2 + a_4)(1 - e^{-a_4\tau})}$$

$$\text{and} \quad A(t,T,u) = A_0(t,T,u) - \lambda\tau(1 + miu) + \lambda \exp\left(iau - \frac{b^2u^2}{2}\right) A_1(t,T,u),$$

where $a_1 = iu(1 - iu)$, $a_2 = i\gamma\rho u - \kappa, a_3 = 1 - i\rho_J\mu_v u$, $a_4 = \sqrt{a_2^2 + a_1\gamma^2}$, $\tau = T - t$, and

$$A_0(t,T,u) = i(r-q)u\tau - \kappa\theta\left(\frac{a_2 + a_4}{\gamma^2}\tau + \frac{2}{\gamma^2}\log\left[1 - \frac{a_2 + a_4}{2a_4}(1 - e^{-a_4\tau})\right]\right),$$

$$A_1(t,T,u) = \frac{a_4 - a_2}{(a_4 - a_2)a_3 + \mu_v a_1}\tau - \frac{2\mu_v a_1}{(a_3a_4)^2 - (a_2a_3 - \mu_v a_1)^2}\log\left[1 - \frac{(a_2 + a_4)a_3 - \mu_v a_1}{2a_3a_4}(1 - e^{-a_4\tau})\right].$$

B.1. The bivariate exponential distribution. The bivariate exponential (BVE) distribution is a bivariate distribution with exponential marginals. It has joint density

$$f(x,y) = \begin{cases} \lambda_2(\lambda_1 + \lambda_{12})\bar{F}(x,y), & x > y, \\ \lambda_1(\lambda_2 + \lambda_{12})\bar{F}(x,y), & x < y, \end{cases}$$

where

(B.2)
$$\bar{F}(s,t) := P(X > s, Y > t) = \exp\left[-\lambda_1 s - \lambda_2 t - \lambda_{12}\max(s,t)\right], \quad s,t > 0.$$

The marginal distribution functions then satisfy $\bar{F}_1(x) = e^{-(\lambda_1+\lambda_{12})x}$ and $\bar{F}_2(y) = e^{-(\lambda_2+\lambda_{12})y}$, and we write $(X,Y) \sim \text{BVE}(\lambda_1, \lambda_2, \lambda_{12})$. The characteristic function for the BVE is given by

(B.3)
$$\int_0^\infty \int_0^\infty e^{isx+ity} dF(x,y) = \frac{(\lambda - is - it)(\lambda_1 + \lambda_{12})(\lambda_2 + \lambda_{12}) + st\lambda_{12}}{(\lambda - is - it)(\lambda_1 + \lambda_{12} - is)(\lambda_2 + \lambda_{12} - it)},$$

where $\lambda := \lambda_1 + \lambda_2 + \lambda_{12}$. Using (B.3) we can calculate the joint characteristic function of $\hat{X}$ in (B.5) to obtain

$$\begin{aligned}\Phi_{\hat{X}}(u_1,u_2;a,b,\lambda_1,\lambda_2,\lambda_{12}) &= \mathbb{E}[\exp((N - E_1)iu_1 + E_2iu_2)] \\ &= \mathbb{E}[\exp(Niu_1)] \cdot \mathbb{E}[\exp(E_1(-iu_1) + E_2(iu_2))] \\ &= \exp\left(aiu_1 - \frac{1}{2}b^2u_1^2\right) \cdot \frac{(\lambda + iu_1 - iu_2)(\lambda_1 + \lambda_{12})(\lambda_2 + \lambda_{12}) - u_1u_2\lambda_{12}}{(\lambda + iu_1 - iu_2)(\lambda_1 + \lambda_{12} + iu_1)(\lambda_2 + \lambda_{12} - iu_2)}.\end{aligned} \tag{B.4}$$

B.2. The jump approximation for the SVCJ model. The goal here is to approximate $X := (X_1, X_2)$ as defined in (5.8) with

$$\hat{X} \;:=\; (N - E_1, E_2), \tag{B.5}$$

where $N \sim \mathrm{N}(a, b)$ and $(E_1, E_2) \sim \mathrm{BVE}(\lambda_1, \lambda_2, \lambda_{12})$ have a BVE distribution (see [17]) that is independent of N. We therefore have five distributional parameters $(a, b, \lambda_1, \lambda_2, \lambda_{12})$ that we can choose in approximating X. Using the BVE distribution also allows us to approximate the variance jumps as well as the correlation between the two components of X in (5.8). If our jump approximation $\hat{X} = (N - E_1, E_2)$ is reasonably accurate, we would expect to have[18]

$$\begin{aligned}
\mathbb{E}(X_1) \approx \mathbb{E}(N - E_1) \;&=\; a - \frac{1}{\lambda_1 + \lambda_{12}} \;=:\; k_1,\\
\mathbb{E}(X_2) \approx \mathbb{E}(E_2) \;&=\; \frac{1}{\lambda_2 + \lambda_{12}} \;=:\; k_2,\\
\mathbb{E}(X_1^2) \approx \mathbb{E}((N - E_1)^2) \;&=\; (a^2 + b^2) - \frac{2a}{\lambda_1 + \lambda_{12}} + \frac{2}{(\lambda_1 + \lambda_{12})^2} \;=:\; k_3,\\
\mathbb{E}(X_1 X_2) \approx \mathbb{E}((N - E_1)E_2) \;&=\; \frac{a}{\lambda_2 + \lambda_{12}} - \frac{1}{\lambda_1 + \lambda_2 + \lambda_{12}} \left(\frac{1}{\lambda_1 + \lambda_{12}} + \frac{1}{\lambda_2 + \lambda_{12}} \right) \;=:\; k_4,\\
\mathbb{E}(X_1^3) \approx \mathbb{E}((N - E_1)^3) \;&=\; (a^3 + 3ab^2) - \frac{3(a^2 + b^2)}{\lambda_1 + \lambda_{12}} + \frac{6a}{(\lambda_1 + \lambda_{12})^2} - \frac{6}{(\lambda_1 + \lambda_{12})^3} \;=:\; k_5.
\end{aligned}$$

We therefore solve[19] the following optimization problem:

$$\begin{aligned}
\min_{a,b,\lambda_1,\lambda_2,\lambda_{12}} \quad & (\mathbb{E}(X_1) - k_1)^2 + (\mathbb{E}(X_2) - k_2)^2 + \left(\mathbb{E}(X_1^2) - k_3\right)^2 + (\mathbb{E}(X_1 X_2) - k_4)^2\\
& + \left(\mathbb{E}(X_1^3) - k_5\right)^2\\
\text{subject to} \quad & b, \lambda_1, \lambda_2, \lambda_{12} \geq 0.
\end{aligned} \tag{B.6}$$

We note that the optimization problem (B.6) is not convex, and so we are only guaranteed to find local minima when we solve it. This was never a problem in the numerical experiments of section 7. We note that it would be easy to automate the process of seeking a good starting point, resolving (B.6), and repeating these two steps until the objective function in (B.6) is sufficiently small.

After solving (B.6) we then use $\hat{X}$ rather than X when modeling the dynamics of L_t. In order to maintain the martingale property of these dynamics, however, we replace m_L in (5.5) with

$$\begin{aligned}
\hat{m} &:= -p^* + (1 - p^*) \cdot \mathbb{E}[\exp(N - E_1) - 1]\\
&= -p^* + (1 - p^*) \left(\exp\left(a^* + \frac{1}{2} b^{*2} \right) \frac{\lambda_1^* + \lambda_{12}^*}{1 + \lambda_1^* + \lambda_{12}^*} - 1 \right),
\end{aligned} \tag{B.7}$$

[18] We note that $\mathbb{E}(\mathrm{E}_1^n) = \frac{n!}{(\lambda_1 + \lambda_{12})^n}$, $\mathbb{E}(\mathrm{E}_2^n) = \frac{n!}{(\lambda_2 + \lambda_{12})^n}$, and $\mathbb{E}(\mathrm{E}_1 \mathrm{E}_2) = \frac{1}{\lambda_1 + \lambda_2 + \lambda_{12}} \left(\frac{1}{\lambda_1 + \lambda_{12}} + \frac{1}{\lambda_2 + \lambda_{12}} \right)$ and use these expressions in our calculations.

[19] As we don't have analytic expressions for $\mathbb{E}(X_1), \mathbb{E}(X_2), \mathbb{E}(X_1^2), \mathbb{E}(X_1 X_2), \mathbb{E}(X_1^3)$, we simply estimated them using Monte Carlo.

where $(a^*, b^*, \lambda_1^*, \lambda_2^*, \lambda_{12}^*)$ is the optimal solution to (B.6). The characteristic function $\Phi_{\hat{X}}(\cdot)$ of $\hat{X}$ is easily computed (see Appendix B.1), which means we can employ the approach of Duffie, Pan, and Singleton [8] to compute the characteristic function of the log-LETF price conditional on $N_1(T) = 0$. This characteristic function may then be used with the Carr–Madan [6] approach to approximate $\hat{C}(L_0, K, T)$.

B.3. The characteristic function of the approximated log-LETF price. The characteristic function of the approximated log-LETF price conditional on $N_1(T) = 0$ is given by

$$\begin{aligned}&\hat{\Phi}_L^{N_1 \equiv 0}(u; \phi, r, q, f, \kappa, \gamma, \theta, V_0, \rho, L_0, \lambda, a, b, \rho_J, \mu_v)\\ &= \exp(\hat{A}(0,T,u) + \hat{B}(0,T,u)\log(L_0) + \hat{C}(0,T,u)V_0^L),\end{aligned}$$

where $\hat{A}, \hat{B}, \hat{C}$ satisfy the ODEs[20]

$$\begin{aligned}\frac{d\hat{B}}{dt} &= 0,\\ \frac{d\hat{C}}{dt} &= -\frac{1}{2}\hat{B}^2 - \hat{B}\hat{C}\rho_L\gamma_L - \frac{1}{2}\hat{C}^2\gamma_L^2 + \frac{1}{2}\hat{B} + \kappa_L\hat{C},\\ \frac{d\hat{A}}{dt} &= -(r - q_L - \lambda\hat{m})C - \kappa_L\theta_L\hat{B} + \lambda_L - \lambda_L \cdot \Phi_{\hat{X}}(u, \hat{B}; \hat{a}, \hat{b}, \lambda_1, \lambda_2, \lambda_{12}),\end{aligned}$$

with boundary conditions $\hat{B}(T,T,u) = iu$, $\hat{C}(T,T,u) = 0$, and $\hat{A}(T,T,u) = 0$, and where

$$\begin{aligned}&(q_L, \kappa_L, \gamma_L, \theta_L, V_0^L, \rho_L, L_0, \lambda_L, \hat{a}, \hat{b}, \lambda_1, \lambda_2, \lambda_{12})\\ &:= (\phi q + f, \kappa, |\phi|\gamma, \phi^2\theta, \phi^2 V_0, \operatorname{sign}(\phi)\rho, L_0, \lambda(1-p^*), a^*, b^*, \lambda_1^*, \lambda_2^*, \lambda_{12}^*).\end{aligned}$$

Note that $\hat{m}$ and $\Phi_{\hat{X}}$ are specified in (B.7) and (B.4). We solved these ODEs, and they have the following explicit solution:

$$\begin{aligned}\hat{B}(t,T,u) &= iu,\\ \hat{C}(t,T,u) &= -\frac{\hat{a}_1(1 - e^{-\hat{a}_3\tau})}{2\hat{a}_3 - (\hat{a}_2 + \hat{a}_3)(1 - e^{-\hat{a}_3\tau})},\\ \hat{A}(t,T,u) &= \hat{A}_0(t,T,u) - \lambda\tau(1 + \hat{m}iu) + \lambda_L \exp\left(\hat{a}iu - \frac{\hat{b}^2u^2}{2}\right)\hat{A}_1(t,T,u),\end{aligned}$$

where $\hat{a}_1 = iu(1 - iu)$, $\hat{a}_2 = \gamma_L\rho_L iu - \kappa_L$, $\hat{a}_3 = \sqrt{\hat{a}_2^2 + \hat{a}_1\gamma_L^2}$, $\tau = T - t$,

$$\alpha(x) = \frac{\hat{a}_3 - \hat{a}_2}{x(\hat{a}_3 - \hat{a}_2) + \hat{a}_1}\tau - \frac{2\hat{a}_1}{(x\hat{a}_3)^2 - (x\hat{a}_3 - \hat{a}_1)^2}\log\left[1 - \frac{(\hat{a}_2 + \hat{a}_3)x - \hat{a}_1}{2\hat{a}_3}(1 - e^{-\hat{a}_3\tau})\right]$$

[20] See Duffie, Pan, and Singleton [8] for the derivation of these ODEs.

and

$$\hat{A}_0(t,T,u) = i(r-q_L)u\tau - \kappa_L\theta_L\left(\frac{\hat{a}_2+\hat{a}_3}{\gamma_L^2}\tau + \frac{2}{\gamma_L^2}\log\left[1-\frac{\hat{a}_2+\hat{a}_3}{2\hat{a}_3}(1-e^{-\hat{a}_3\tau})\right]\right),$$

$$\hat{A}_1(t,T,u) = \alpha(\lambda_2+\lambda_{12})\cdot\frac{\lambda_2+\lambda_{12}}{(\lambda_1+\lambda_{12}+iu)(\lambda_1+iu)}\left[(\lambda_1+\lambda_{12})(\lambda_1+iu)+iu\lambda_{12}\right]$$
$$-\alpha(\lambda_1+\lambda_2+\lambda_{12}+iu)\cdot\frac{iu\lambda_{12}(\lambda+iu)}{(\lambda_1+\lambda_{12}+iu)(\lambda_1+iu)}.$$

Appendix C. Additional numerical results.

C.1. Jump approximation parameters for the SVCJ model. We report in Table 12 the jump approximation parameters for the SVCJ model that we obtained by solving the optimization problem of Appendix B.2. These parameter values were used to obtain C_{tran} for the SVCJ model in section 7 (parameter sets II and III) and Appendix C.2 (parameter set I).

C.2. Results for parameter set I. We report in Tables 13 to 15 our numerical results for the low-volatility environment of parameter set I. We see that there is very little variation in LETF option prices and implied volatilities across the three models. In addition, the Monte Carlo prices are very close to the prices obtained via numerical transform inversion for each model.

Table 12
Optimized jump approximation parameters for the SVCJ model.

Parameter set	Leverage ratio	SVCJ model				
	ϕ	a^*	b^*	λ_1^*	λ_2^*	λ_{12}^*
I	2	0.0641	0.2114	0.9571	17.3016	7.4705
	3	0.2524	0.1910	0.1112	8.6678	2.6477
	−1	0.0484	0.1113	0.1112	59.6036	23.4571
	−2	0.1315	0.2163	0.2282	14.9813	6.9231
	−3	0.4228	0	0.0193	9.1694	2.1501
II	2	0.2225	0.5919	0.8507	2.5896	0.1404
	3	0.5192	0.6608	0.8826	1.1648	0.0719
	−1	0.6063	0.0009	0	8.5916	2.1552
	−2	0.9422	0	1.5352	2.5810	0
	−3	1.2021	0.0003	1.3639	1.1316	0
III	2	0.0204	0.4170	1.0564	6.7329	0
	3	0.1580	0.5781	0.9774	2.9885	0
	−1	0.3766	0	0	12.3884	6.3770
	−2	0.8057	0	2.0278	6.6275	0
	−3	1.0509	0	1.6341	2.9142	0

Table 13

Option prices on underlying index/ETF for parameter set I computed via Monte Carlo and transform inversion approaches. Approximate 95% confidence intervals are reported in brackets.

Moneyness	BS vol(%)	BS price	Option price (SV)		Option price (SVJ)		Option price (SVCJ)	
$\frac{K}{S_0}$	Σ_{BS}	C_{BS}	C_{sim}	C_{tran}	C_{sim}	C_{tran}	C_{sim}	C_{tran}
0.85	21.47	16.37	16.38	16.38	16.37	16.37	16.37	16.37
			[16.38, 16.38]	-	[16.37, 16.37]	-	[16.37, 16.37]	-
1	20.17	5.92	5.99	5.99	5.92	5.92	5.94	5.94
			[5.99, 5.99]	-	[5.92, 5.92]	-	[5.94, 5.94]	-
1.15	19.20	1.23	1.27	1.27	1.22	1.22	1.23	1.23
			[1.27, 1.27]	-	[1.22, 1.22]	-	[1.23, 1.23]	-

Table 14

Comparison of Black–Scholes implied volatilities: Parameter set I.

Leverage ratio	Moneyness		Implied volatility (SV)			Implied volatility (SVJ)			Implied volatility (SVCJ)		
ϕ	$\frac{K_S}{S_0}$	$\frac{K_L}{L_0}$	Σ_S	Σ_L	$\frac{\Sigma_L}{\Sigma_S}$	Σ_S	Σ_L	$\frac{\Sigma_L}{\Sigma_S}$	Σ_S	Σ_L	$\frac{\Sigma_L}{\Sigma_S}$
2	0.85	0.7	21.51	43.11	2.00	21.43	43.14	2.01	21.43	43.21	2.02
	1	1	20.41	40.66	1.99	20.17	40.22	1.99	20.22	40.33	1.99
	1.15	1.3	19.44	38.82	2.00	19.18	38.26	1.99	19.24	38.41	2.00
3	0.85	0.55		64.92	3.02		65.48	3.06		65.22	3.04
	1	1		60.79	2.98		60.26	2.99		60.27	2.98
	1.15	1.45		58.17	2.99		57.30	2.99		57.48	2.99
−1	0.85	1.15		21.43	1.00		21.20	0.99		21.25	0.99
	1	1		20.49	1.00		20.21	1.00		20.28	1.00
	1.15	0.85		19.39	1.00		19.27	1.00		19.25	1.00
−2	0.85	1.3		42.91	1.99		42.38	1.98		42.51	1.98
	1	1		41.16	2.02		40.60	2.01		40.75	2.02
	1.15	0.7		38.77	1.99		38.81	2.02		38.64	2.01
−3	0.85	1.45		64.45	3.00		63.59	2.97		63.82	2.98
	1	1		62.00	3.04		61.18	3.03		61.40	3.04
	1.15	0.55		58.04	2.99		58.82	3.07		58.24	3.03

Table 15

Comparing leveraged ETFs option prices with approximate prices in parameter set I. Approximate 95% confidence intervals are reported in brackets.

Leverage ratio	Moneyness		Option price (SV)		Option price (SVJ)		Option price (SVCJ)	
ϕ	$\frac{K_S}{S_0}$	$\frac{K_L}{L_0}$	C_{sim}	C_{tran}	C_{sim}	C_{tran}	C_{sim}	C_{tran}
2	0.85	0.7	31.81	31.80	31.81	31.81	31.82	31.79
			[31.80, 31.81]	-	[31.80, 31.81]	-	[31.81, 31.82]	-
	1	1	11.65	11.65	11.53	11.53	11.56	11.55
			[11.65, 11.66]	-	[11.53, 11.54]	-	[11.56, 11.57]	-
	1.15	1.3	2.91	2.91	2.80	2.80	2.83	2.84
			[2.91, 2.91]	-	[2.79, 2.80]	-	[2.82, 2.83]	-
3	0.85	0.55	46.75	46.74	46.80	46.79	46.78	46.76
			[46.74, 46.76]	-	[46.79, 46.81]	-	[46.77, 46.78]	-
	1	1	17.23	17.21	17.08	17.07	17.08	17.05
			[17.22, 17.23]	-	[17.07, 17.09]	-	[17.08, 17.09]	-
	1.15	1.45	4.98	4.98	4.79	4.79	4.83	4.81
			[4.97, 4.98]	-	[4.78, 4.79]	-	[4.82, 4.83]	-
−1	0.85	1.15	1.66	1.66	1.61	1.61	1.62	1.64
			[1.66, 1.66]	-	[1.61, 1.61]	-	[1.62, 1.62]	-
	1	1	6.01	6.01	5.93	5.93	5.95	5.96
			[6.01, 6.02]	-	[5.93, 5.94]	-	[5.95, 5.96]	-
	1.15	0.85	16.10	16.10	16.09	16.08	16.08	16.08
			[16.10, 16.10]	-	[16.08, 16.09]	-	[16.08, 16.08]	-
−2	0.85	1.3	3.78	3.80	3.67	3.67	3.69	3.76
			[3.78, 3.78]	-	[3.66, 3.67]	-	[3.69, 3.70]	-
	1	1	11.79	11.79	11.64	11.63	11.68	11.72
			[11.79, 11.80]	-	[11.63, 11.64]	-	[11.67, 11.68]	-
	1.15	0.7	31.34	31.33	31.35	31.33	31.33	31.33
			[31.34, 31.35]	-	[31.34, 31.35]	-	[31.32, 31.34]	-
−3	0.85	1.45	6.43	6.46	6.23	6.24	6.28	6.31
			[6.43, 6.44]	-	[6.22, 6.23]	-	[6.28, 6.29]	-
	1	1	17.56	17.55	17.33	17.31	17.39	17.41
			[17.55, 17.56]	-	[17.33, 17.34]	-	[17.39, 17.40]	-
	1.15	0.55	46.22	46.20	46.27	46.25	46.23	46.25
			[46.21, 46.22]	-	[46.26, 46.28]	-	[46.22, 46.24]	-

REFERENCES

[1] L. Andersen, *Efficient Simulation of the Heston Stochastic Volatility Model*, January 2007; available online from http://papers.ssrn.com/sol3/papers.cfm?abstract_id=946405.

[2] M. Avellaneda and S. Zhang, *Path-dependence of leveraged ETF returns*, SIAM J. Financial Math., 1 (2010), pp. 586–603.

[3] O. E. Barndorff-Nielsen and N. Shephard, *Non-Gaussian Ornstein-Uhlenbeck-based models and some of their uses in financial economics*, J. R. Stat. Soc. Ser. B Stat. Methodol., 63 (2001), pp. 167–241.

[4] D. Bates, *Exchange rate processes implicit in Deutsche mark options*, Rev. Financial Stud., 7 (1996), pp. 69–107.

[5] M. Broadie and A. Jain, *Pricing and hedging volatility derivatives*, J. Derivatives, 15 (2008), pp. 7–24.

[6] P. Carr and D. Madan, *Option valuation using the fast Fourier transform*, J. Comput. Finance, 2 (1998), pp. 61–73.

[7] M. Cheng and A. Madhavan, *The dynamics of leveraged and inverse exchange traded funds*, J. Investment Management, Winter 2009 (2009).
[8] D. Duffie, J. Pan, and K. Singleton, *Transform analysis and asset pricing for affine jump-diffusions*, Econometrica, 68 (2000), pp. 1343–1376.
[9] Chicago Board Options Exchange, *CBOE 2013 Market Statistics*, 2013; available online from http://www.cboe.com/data/marketstats-2013.pdf.
[10] P. Glasserman and K. Kim, *Saddlepoint approximations for affine jump-diffusion models*, J. Econom. Dynam. Control, 33 (2009), pp. 37–52.
[11] P. Glasserman and K. Kim, *Saddlepoint approximations for affine jump-diffusion models*, J. Econom. Dynam. Control, 33 (2009), pp. 15–36.
[12] P. Glasserman and N. Merener, *Cap and swaption approximations in Libor market models with jumps*, J. Comput. Finance, 7 (2003), pp. 1–36.
[13] M. B. Haugh, *A note on constant proportion trading strategies*, Oper. Res. Lett., 39 (2011), pp. 172–179.
[14] M. B. Haugh and A. Jain, *The dual approach to portfolio evaluation: A comparison of the static, myopic and generalized buy-and-hold strategies*, Quant. Finance, 11 (2011), pp. 81–99.
[15] S. Heston, *A closed-form solution for options with stochastic volatility with applications to bond and currency options*, Rev. Financial Stud., 6 (1993), pp. 327–343.
[16] T. Leung and R. Sircar, *Implied volatility of leveraged ETF options*, Appl. Math. Finance, 22 (2015), pp. 162–188.
[17] A. W. Marshall and I. Olkin, *A multivariate exponential distribution*, J. Amer. Statist. Assoc., 62 (1967), pp. 30–44.
[18] J. Zhang, *Path Dependence Properties of Leveraged Exchange-Traded Funds: Compounding, Volatility and Option Pricing*, Ph.D. thesis, NYU, 2010.
[19] J. Zhu, *Applications of Fourier Transform to Smile Modeling*, Springer, New York, 2010.